



**Boston University Department of Mechanical Engineering:  
ME460/461 Capstone Experiences**

## **Semester 2 Final Report**

**Team 31: Gas Turbine From Turbocharger**



**Team Members:**

*Nathan Lau*

*Noel Cummings*

*Jason Cruz*

**With Contributions From:**

*Hector Castro Noguez*

Date: April 28, 2024

Project Advisor: *Prof. Frank DiBella*

Client: *Prof. Anthony Linn*

## Table of Contents

<b>1 Executive Summary.....</b>	<b>3</b>
1.1 Project Overview.....	3
1.1.1 Nathan Lau.....	3
1.1.2 Noel Cummings.....	3
1.1.3 Jason Cruz.....	3
<b>2 Introduction and Background.....</b>	<b>4</b>
2.1 Overview.....	4
2.2 Problem Statement.....	4
2.3 Basics of an Automotive Turbocharger.....	4
2.4 Basics of Combustion Chambers.....	6
2.5 Flame Tube Zones for Air/Fuel Micromixing.....	8
2.6 Electrical Generators.....	9
2.7 Brayton Cycle Analysis.....	10
<b>3 Customer Requirements.....</b>	<b>13</b>
3.1 Background.....	13
3.2 Key Findings.....	14
3.3 Engineering Specifications.....	14
<b>4 System Design.....</b>	<b>16</b>
4.1 Early Stage Combustion Chamber and Flame Tube Design.....	16
4.2 Late Stage Combustion Chamber and Flame Tube Design.....	17
4.3 Electric Generator in Parallel (Pulley System).....	18
4.3.1 Pulley: Generator Assembly Design.....	18
4.3.2 Mesh Guard.....	21
4.4 Carriage/Cart Design.....	21
4.4.1 Overview.....	21
4.4.2 Initial Design Stage.....	22
4.4.3 Later Design Stage.....	23
4.4.4 Final Design.....	24
4.4.5 Materials.....	24
4.4.6 Structural Analysis of the Cart.....	25
4.5 Mounting Points for the Turbocharger.....	27
4.6 Pipe Configuration.....	30
4.7 Final Gas Turbine System.....	31
4.8 Electrical System.....	32
4.8.1 Instrumentation.....	33
4.8.2 Controls and Safety Measures.....	36
4.9 Cooling System.....	38

4.10 Air Start System.....	41
4.11 Fuel Flow Sizing.....	44
<b>5 Feasibility Analysis.....</b>	<b>44</b>
5.1 Combustion Chamber Compressor Flow Analysis (no combustion).....	44
5.2 Revised Combustion Chamber Compressor Flow Analysis (no combustion).....	46
5.3 Combustion Analysis of the Flame Tube Design.....	47
<b>6 Conclusion.....</b>	<b>48</b>
<b>7 Further Works.....</b>	<b>49</b>
7.1.1 Hybrid Turbochargers (MGU-H).....	49
7.1.2 Electric Generator Concept in Series (MGU-H).....	50
7.2 Scale Prototype Combustion Chamber Model.....	51
<b>References.....</b>	<b>53</b>
<b>Appendices.....</b>	<b>55</b>
Bill of Materials (BOM).....	55
Combustion Chamber and Motor-Pulley.....	55
Oil Loop.....	57
Coolant Loop.....	57
Cart Extrusions.....	58
Cart Fasteners.....	59
Pipe and Tubes.....	60
Misc Cart Parts.....	61
Air Start System.....	62
Fuel.....	63
Instrumentation and Data.....	64
Electrical.....	66

# **1 Executive Summary**

## **1.1 Project Overview**

Boston University's mechanical engineering professors are currently looking for a way to demonstrate compressible flow principles in a laboratory setting. At the moment, there is no equipment available to provide data for flow analyses of turbomachinery components. The solution presented involves converting an automotive turbocharger into a small, mobile gas turbine engine through the addition of a combustion chamber and other necessary subsystems: oil lubrication, water cooling, instrumentation, etc. The inclusion of a generator attached to the turbocharger shaft for low power generation is another key design factor.

### **1.1.1 Nathan Lau**

Nathan was primarily responsible for designing the combustion chamber (with help from Jason), parts of the turbocharger, as well as the dual pulley design for the motor/generator unit. Analysis of the combustor system was conducted using CFD software from SolidWorks as well as SimFlow CFD to iterate on the flame tube archetype along with the pulley assembly to calculate the tension ratio as a safety measure. Lastly, the scaled prototype combustion system was designed, sourced, and manufactured predominantly by myself.

### **1.1.2 Noel Cummings**

Noel was primarily responsible for designing the instrumentation and controls system for the gas turbine system. This included choosing the correct data acquisition system for a classroom setting and choosing the correct sensors based on the temperatures and pressures throughout the cycle. He was also responsible for modeling the gas turbine as a Brayton Cycle so a design point could be picked from the turbocharger compressor map, carrying out heat exchanger analysis to source the cooling system, and refining the air start system.

### **1.1.3 Jason Cruz**

Jason was in charge of designing the cart, as well as working on the combustion chamber with Nathan. For the cart, this involved a variety of sketches and measurements to scale a cart that can both fit the entire gas turbine system but also be transportable and be able to fit through a standard door and inside an elevator. In addition an FEA analysis of the cart structure was conducted as well. The combustion chamber involved both sketches, modeling, and running some CFD simulations in order to determine airflow. Additionally assisted with CAD modeling components of the provided turbocharger to be used for the CAD of the complete system.

## **2 Introduction and Background**

### **2.1 Overview**

The aim of this project was to demonstrate a gas turbine system as a way to promote engagement with students. The process involved the transformation of an automotive turbocharger into a fully moveable and simple to use gas turbine system that is capable of measuring the pressures, flow rates, temperatures, and speeds of the device. An analytical system is used to calculate efficiencies and output power to be displayed to the end user.

A key concept pertaining to this project is the Brayton Cycle. Understanding the Brayton Cycle is crucial for many inventions that are used in transportation and energy production industries. From the internal combustion engine (ICE) in cars, gas turbine power plants, and to the jet engines used in airplanes, the Brayton Cycle's fundamentals can be found everywhere. Understanding its theory is essential to the engineer looking to develop their skills and knowledge in this field. Therefore, being able to bring this technology to the classroom setting in a safe measure better enhances the learning experience of the students which, in turn, benefits the College of Engineering Department at Boston University.

### **2.2 Problem Statement**

Boston University's mechanical engineering department currently lacks sufficient equipment to physically demonstrate compressible flow and propulsion principles to students interested in aerospace and fluids. Over the past few years, no new resources have been created for incoming classes of students taking the aerospace engineering concentration. Therefore, students don't have the chance to interact with real systems and learn how propulsion systems change throughout a cycle and react with parameter changes. Being able to engage through a variety of mediums and allowing students to physically interact with equipment better the quality of learning for the individual. Creating a demonstration of gas turbine principles would give students valuable experience with a system they may work with in the future.

### **2.3 Basics of an Automotive Turbocharger**

While combustion engines as a technology in the automotive industry have had years of refinement, fundamental flaws still exist inherent to its design. A phenomenon called "knocking", an occurrence of the irregularity of fuel burning in the combustion chamber may occur. This is when the fuel-to-air mixture ratio is uneven in each cylinder per cycle of the engine. As a result, the engine can run "lean" meaning there is too much air, or "rich" where there is too much fuel. This inconsistency in combustion hurts the efficiency of an engine which negatively impacts the fuel economy. Thus, it is the goal of a turbocharger to supply an engine with a consistent supply of air to a complete combustion.

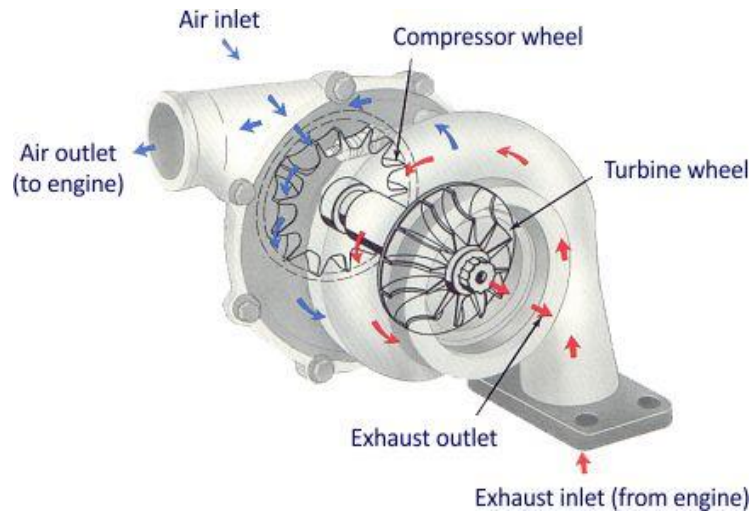


**Figure 1.** Diagram of a Turbocharger (compressor and turbine)  
(Source: Schwitzer)

A turbocharger comprises a turbine and a compressor which works to compress air to help aid the combustion cycle in an automotive engine. Energy from exhaust gasses that would've been wasted is instead used to power the turbine of the turbocharger. An extended shaft connects the turbine (the hot end) to the compressor (the cold end) which compresses air from the ambient environment to feed into the intake manifold of the engine.

As a part of the turbocharger's design is a wastegated system for relieving pressure. This component of the turbocharger is necessary for the longevity of the device as when a driver is off-throttle, the exhaust gasses are still powering the turbine, but the engine is not powering the crankshaft and doesn't require the compression of air. Thus, a wastegate opens on the turbine side to relieve pressure and prevents the turbocharger from failure. The turbocharger supplied for this project uses a different device to achieve a similar result. The Garrett GT3788VA Turbocharger, the part used for this project, is a Variable Geometry Turbocharger (VGT).

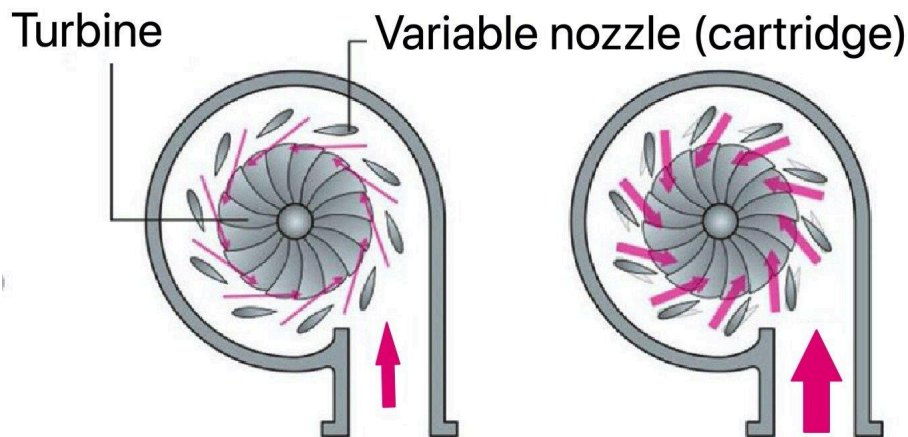


**Figure 2.** Diagram of Variable Geometry Turbocharger (VGT)

The vanes (or fins) of a variable geometry turbocharger can dynamically change its orientation to affect the flow of exhaust gasses flowing through the turbine. When the vanes are closed (see Figure 2. (left)), the exhaust gas is more restricted which suppresses the flow and the turbine's rotational speed decreases. When the vanes are open, the exhaust flow is unrestricted which increases the rotational speed of the turbine.<sup>1</sup> This system is controlled by a sensor that detects the angle of the vanes and a solenoid that shifts a plate connecting all the vanes. This solution is more precise in relieving pressure compared to a traditional wastegate but consumes more oil to maintain.

## 2.4 Basics of Combustion Chambers

The combustion chamber is one of the most important aspects of any gas turbine system. In a traditional gas turbine system, the combustion chambers play the role of being the main energy provider. The process begins with a starter system that allows the compressor to begin spinning. This starting process can be achieved in a variety of ways including through an air starter, electrical starter via an APU, or even hydraulic pumps and motors. After the system is started, the compressor begins to spin and starts to pull in air via the front of the gas turbine. This air is then compressed into several stages of compressors until it reaches the combustor where jet fuel is sprayed and mixed with the inflow of compressed air. This mixture is ignited and a stream of very hot gasses flows through a turbine that then spins and continues the entire cycle. This entire process can be described by the Brayton Cycle, which explains the entire cycle that the system undergoes during its function. The hot gasses then exit through the turbine and can then be used for such applications like thrust in aerospace applications or to power a generator for industrial uses.

There are several types of combustion chambers which are categorized into three main types: can, can-annular, and annular.<sup>2</sup> Can type combustors consist of a ring of self contained cylinders surrounding the gas turbine. Each of these cylinders features its own igniters, casing, liners, and fuel injectors. Can-annular type combustors are similar to can-types where it consists of having its own set of components as featured within the can-types with the main difference coming from its layout being more integrated into one entire ring rather than separate cylinders arranged in a ring like orientation. The annular type replaces the separate combustion zones in favor of a continuous liner in the shape of a ring. Among these three types, the most simple and often used is the annular type in part due to it having such advantages as having more uniform combustion, and being generally smaller in dimension thanks to its geometry.

---

<sup>1</sup> H. Arimizu, et al., "Development of Variable Geometry Turbocharger for Gasoline Engine." *Mitsubishi Heavy Industries*, 2012.

<sup>2</sup> Arnedo, Manuel Soler. "6.2.4: Combustion Chamber." *Engineering LibreTexts*, Libretexts, 21 Jan. 2022, [eng.libretexts.org/Bookshelves/Aerospace\\_Engineering/Fundamentals\\_of\\_Aerospace\\_Engineering\\_\(Arnedo\)/06%3A\\_Aircraft\\_propulsion/6.02%3A\\_The\\_jet\\_engine/6.2.04%3A\\_Combustion\\_chamber](https://eng.libretexts.org/Bookshelves/Aerospace_Engineering/Fundamentals_of_Aerospace_Engineering_(Arnedo)/06%3A_Aircraft_propulsion/6.02%3A_The_jet_engine/6.2.04%3A_Combustion_chamber).

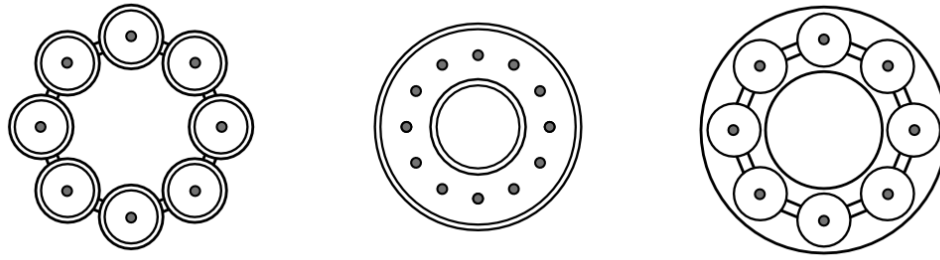


**Figure 3.** Cross sectional views of the three types of combustion chambers (From left to right: Can, Annular, Can-Annular)

An intricate and equally important aspect of the combustor is the need for proper mixing of fuel and air as well as cooling throughout the combustion process to ensure overheating doesn't occur. This can be achieved through the presence of holes within the inner liner of the combustors. For most combustion chambers, there are several sections where these holes are placed. The first area is called the primary zone where the main source of compressed air is mixed with fuel and then combusted. The next zone is called the intermediate zone where the combustion process is often completed via air that flows through the second set of holes. This is then followed by a tertiary zone called the dilution zone where the compressed air is used primarily for the purpose of cooling the hot gasses before it reaches the turbine.<sup>3</sup>

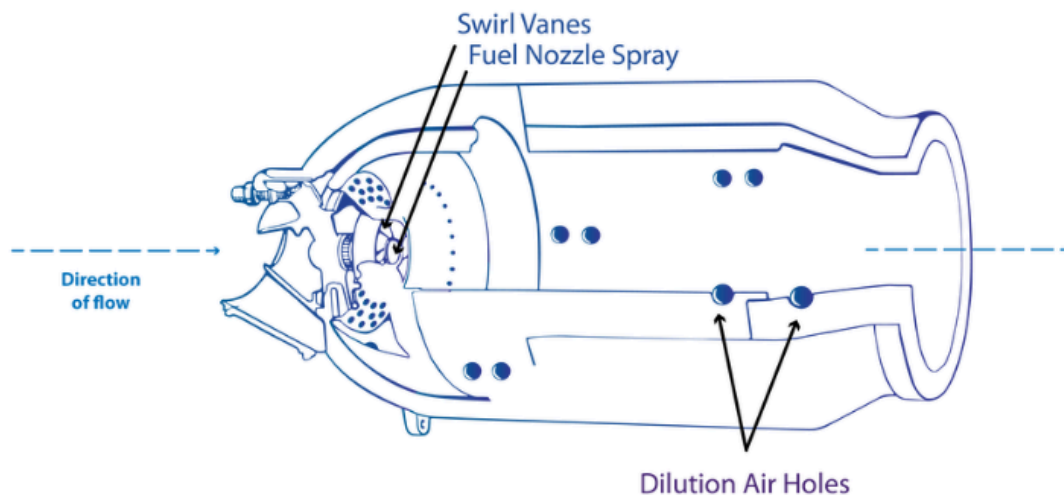


**Figure 4.** Diagram of a gas turbine combustion chamber. Notice the presence of dilution holes.

Since the main aspect of this project is to adapt an automotive turbocharger into a gas turbine system, the combustion chamber will play a particularly important role as it will be in

<sup>3</sup> Lefebvre, Arthur H., and Dilip R. Ballal. "Basic Considerations." *Gas Turbine Combustion Alternative Fuels and Emissions*, Taylor & Francis, Boca Raton u.a., FL, 2010, pp. 15–17.

place of the piston engine. Like with a piston engine, the hot exhaust gasses from the combustion chamber will be used to drive the turbine which in turn will spin the compressor to pull in more air, thus maintaining the process until either the fuel within the combustion chamber runs out or the system is shut off.

## 2.5 Flame Tube Zones for Air/Fuel Micromixing

The development of the combustion chamber to improve its efficiency focused on the flame tube design with the configuration of the holes used to dilute the air/fuel mixture during combustion. In many cases of flame tube combustors, it was found that the most difficult part was the initial ignition of the system. Often, the flame would be blown out before the flame could be self sufficient. Thus, decreasing the total area of the primary zone holes in relation to the secondary and tertiary zones was to help recirculation to adequately facilitate the mixing of the air and fuel.<sup>4</sup> This was achieved as the high velocity air from the compressor flowing through the flame tube holes would create micro zones of recirculation which promotes the micromixing for a more complete combustion. Since there is high pressure on the outer surface of the flame tube, low pressure is generated on the inner surface adjacent to the hole (near the vena contracta). The low pressure pulls the high velocity air flow outward to create small areas of circulation (see Figure below).

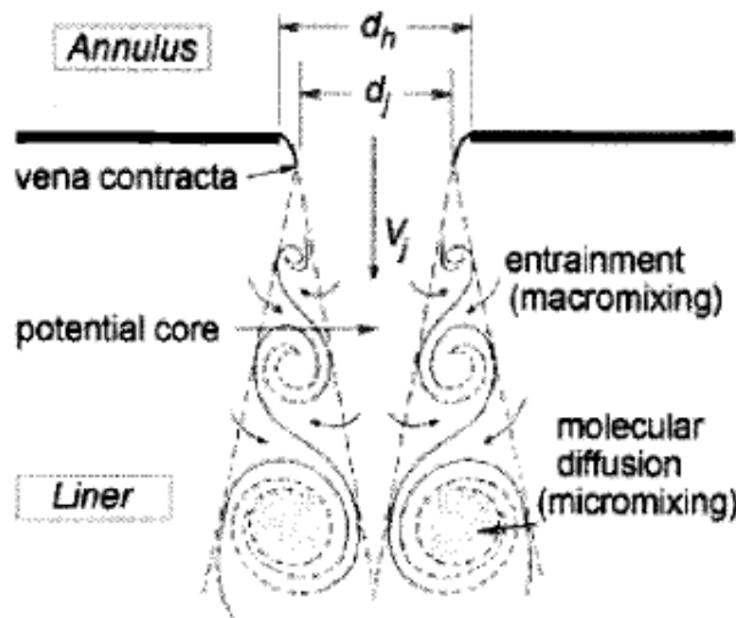


**Figure 5.** Fluid micromixing through annulus holes in the flame tube to encourage complete combustion

<sup>4</sup> John Kyle Thoma, et al., "Design, Fabrication, and Testing of an Automotive Turbocharger-Based Gas Turbine Engine", California Polytechnic State University, San Luis Obispo, June 2010.

As the hole diameter ( $d_h$ ) decreases, the velocity gradient across the diameter of the hole diminishes to limit the high energetic air from disrupting the flame inside. Thus, for more refined air/fuel micromixing, the primary zone would need to feature many tiny holes. Contrastingly, the following zones don't need to facilitate micromixing as much as the primary zone, thus the secondary and tertiary zones would feature larger but fewer holes.

For the secondary zone, its primary purpose is to complete the combustion from the products from the primary zone. The secondary zone is located further down the flame tube as the inlet from the compressor introduces air between the two zones instead of directly onto either zone. It keeps temperatures in check so that there exists enough heat to stabilize the flame but not too hot that the flame tube material is damaged. As a result, the holes in the secondary zone are slightly larger in diameter than the primary zone, but feature less holes and less total area. This is because the combustion (in theory) is mostly complete and the fuel particles as a result from incomplete combustion requires more micromixing to achieve complete combustion to improve the efficiency of the device.

Lastly, the tertiary zone located at the end of the flame tube is meant to remove any hot spots exiting the combustion chamber and into the turbine. The remaining cooler air between the flame tube and the combustion chamber walls then mixes through large holes with the hot expanding gasses. This would benefit the longevity of the components by preventing excessive heat stress on the materials further along the pipe and into the turbine.

## 2.6 Electrical Generators

An electrical generator is a device that is used to convert various forms of energy such as mechanical energy or fuel based energy into electricity that can then be used to power external appliances<sup>5</sup>. The mechanical energy can either come from kinetic (motion based) or potential energy (stored) and common sources of these types of energies include steam turbines, gas turbines, and wind turbines. For generators, the basic principle in which they function is the electromagnetic induction principle in which an electric current is created by moving a wire besides a magnet.

Electric generators can either be rotating based or static. Rotating electric generators can be categorized into two types: a dynamo or an alternator. Dynamos operate by generating pulsing direct currents through a commutator. These types of generators were the earliest forms that were capable of delivering vast amounts of electricity to appliances and provided a foundation for which many other electric to power conversion devices are based on. In the present day these forms are now obsolete. On the other hand alternators operate by generating alternating currents. Most generators used to supply electrical energy to national grids today are alternators. In both cases, three main components of a generator that are needed to generate electricity are a wire, a

---

<sup>5</sup> "U.S. Energy Information Administration - EIA - independent statistics and analysis," How electricity is generated - U.S. Energy Information Administration (EIA), <https://www.eia.gov/energyexplained/electricity/how-electricity-is-generated.php> (accessed Apr. 28, 2024).

magnetic field, and relative motion between the wire and the magnetic field.

For the purpose of this project, rotating based generators will be the main focus as the team will be using an induction motor. Induction motors consist of a rotor (the part that rotates, usually made with electromagnets) and a stator (stationary part that surrounds the rotor). In standard conditions, the induction motor operates by having an alternating current supplied to the motor's stator which in turn creates a rotating magnetic field that induces current onto the rotor. The induced current on the rotor also creates a magnetic field which causes it to follow the stator due to attraction from the magnetic field. However, the rotor will be rotating at a slower rate than the field created by the stator which causes slip to occur. The figure below shows an example of an induction motor.



**Figure 6.** A 3 phase induction motor.

The induction motor can be turned into an induction generator if the rotor is mechanically spun faster than its synchronous speed. To do this a prime mover ( such as a turbine or engine) drives the rotor at a rate that's beyond its synchronous speed which causes negative slip to occur.

## 2.7 Brayton Cycle Analysis

The analysis of a gas turbine system begins with understanding the basic thermodynamic principles behind it. As an air-breathing device, a gas turbine can be analyzed using a Brayton cycle model. Figure 7 shows a basic open Brayton Cycle, and Figure 8 shows the temperature-enthalpy diagram that describes an ideal version of the system in Figure 7.

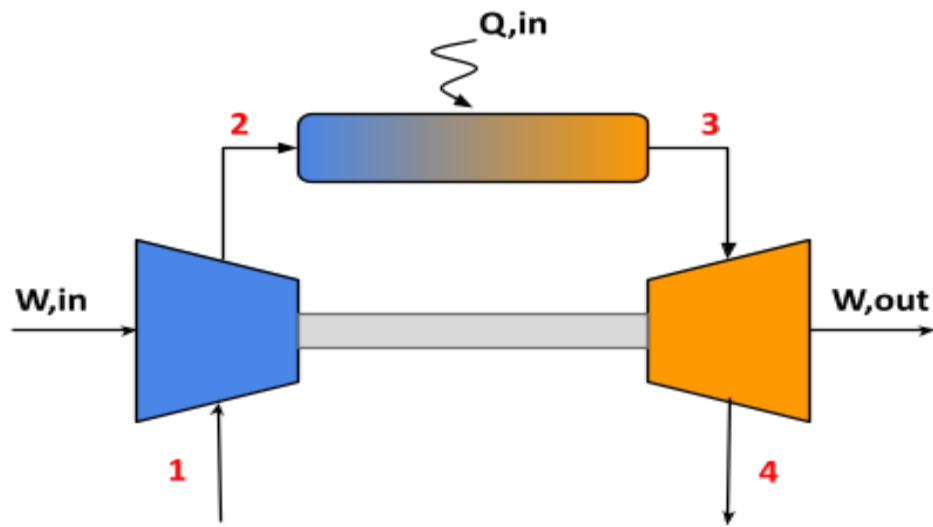


**Figure 7.** Diagram of an open Brayton Cycle showing inputs and outputs

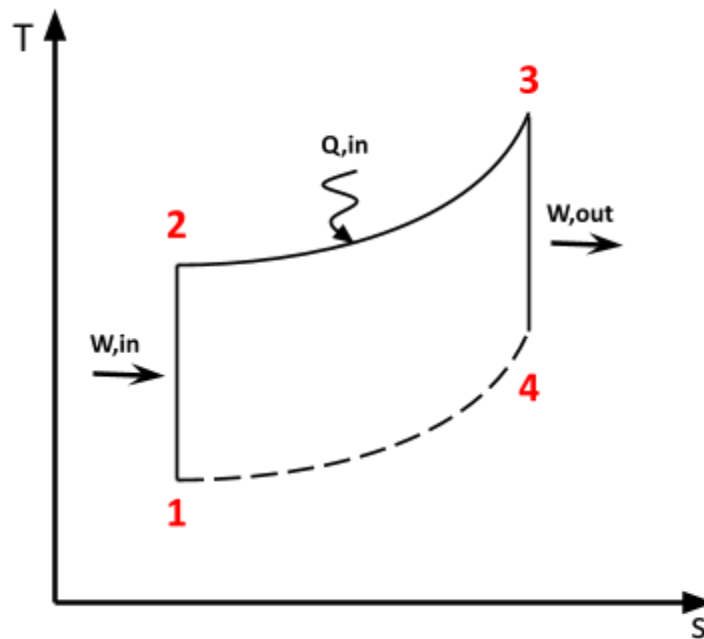


**Figure 8.** Temperature-enthalpy diagram showing the heat and work inputs and outputs of an ideal Brayton Cycle

Process 1-2 is isentropic compression through the compressor, Process 2-3 is heat addition through the combustor, Process 3-4 is isentropic expansion, and Process 4-1 is heat rejection to the atmosphere. The line for Process 4-1 is not solid because the system is open: air enters and is exhausted to atmospheric conditions. Even though the system is open, the same analysis can be done since 4-1 is an isobaric process.

The static temperature at State 2 can be found for a real compression process using Equation 1.

$$T_2 = \frac{T_1 \left( \frac{P_2}{P_1} \right)^{\frac{\gamma-1}{\gamma}} - T_1}{\eta_c} + T_1 \quad (1)$$

where  $\gamma$  is the ratio of specific heats ( $\gamma=1.4$  for air) and  $\eta_c$  is the isentropic efficiency of the compressor.  $T_1$  and  $P_1$  are set by atmospheric conditions, and  $\frac{P_2}{P_1}$  is set by a design point chosen from the turbocharger compressor map. For the Garrett GT3788VA turbocharger used in this project, the compressor map is shown in Figure 9.

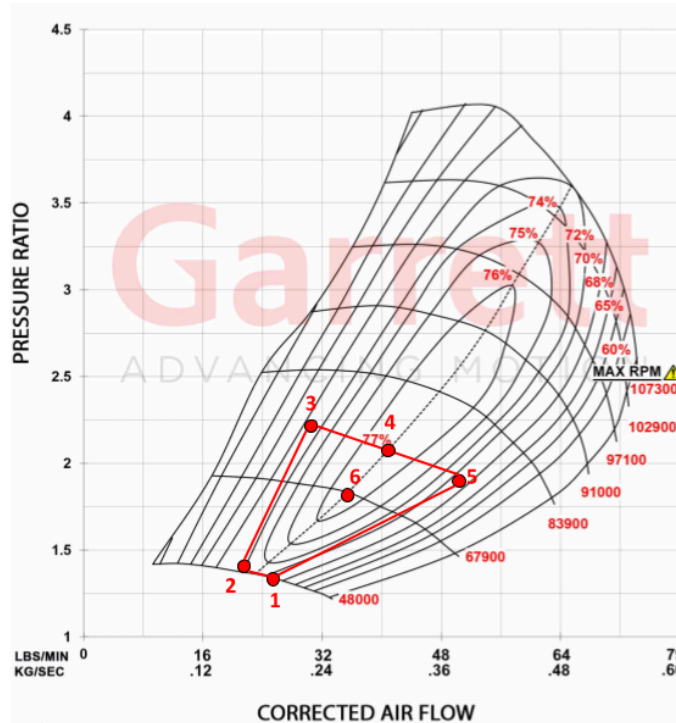


**Figure 9.** Compressor performance map for Garrett GT3788VA turbocharger with select design points

Choosing a design point from the map gives pressure ratio, air mass flow, and turbocharger rotational speed values. For this analysis, the team picked Point 6 as the design point. For this point, the pressure ratio is 1.8, the mass flow rate ( $\dot{m}$ ) is  $0.583 \frac{lbm}{s}$ , the rotational speed is 67900 RPM, and the efficiency is 0.77. The pressure ratio is used to find  $T_2$ , and the mass flow can be used to find the energy added through combustion.

The combustion process is described by Equation 2:

$$\dot{Q}_{23} = \dot{m} c_p (T_3 - T_2) \quad (2)$$

where  $c_p$  is the specific heat at constant pressure and is  $0.24 \frac{Btu}{lbmR}$  for air. For the design process,  $T_3$  was chosen based on commonly quoted values for the max exhaust gas temperature (1250°F). The required fuel mass flow rate can be calculated by dividing the heat addition calculated using Equation 2 by the higher heating value of propane ( $\Delta H = 21700 \frac{Btu}{hr}$ ).

$$\dot{m}_f = \frac{\dot{Q}_{23}}{\Delta H} \quad (3)$$

The higher heating value assumes that any water vapor remains liquid throughout combustion, so no heat is lost to phase change.

The static exhaust temperature can be found using Equation 4

$$T_4 = T_3 - T_3 \left(1 - \left(\frac{P_4}{P_3}\right)^{\frac{\gamma-1}{\gamma}}\right) \eta_t \quad (4)$$

In this analysis,  $P_4$  is assumed to be atmospheric,  $P_3 = P_2$ , assuming no pressure loss in the combustor, and  $\eta_t$  is the isentropic efficiency of the turbine.

Using the state values, the power used by the compressor and generated by the turbine are calculated. The compressor work is given by Equation 5.

$$\dot{W}_{12} = \dot{m} c_p (T_2 - T_1) \quad (5)$$

The turbine work is given by Equation 6.

$$\dot{W}_{34} = \dot{m} c_p (T_3 - T_4) \quad (6)$$

For the design point, the analysis using the above equations (with  $\eta_c = 0.77$  and  $\eta_t = 0.75$ ) yields the following results:  $T_1 = 60.3^\circ F$ ,  $P_1 = 14.7 \text{ psia}$ ,  $T_2 = 183.3^\circ F$ ,  $P_2 = 26.5 \text{ psia}$ ,  $T_3 = 1250^\circ F$ ,  $P_3 = 26.5 \text{ psia}$ ,  $T_4 = 1051^\circ F$ ,  $P_4 = 14.7 \text{ psia}$ ,  $\dot{W}_{12} = 24 \text{ hp}$ ,  $\dot{W}_{34} = 39 \text{ hp}$ ,  $\dot{W}_{net} = 15 \text{ hp}$ ,  $\dot{Q}_{23} = 5.4E5 \text{ Btu/hr}$ ,  $\dot{m}_f = 0.00687 \text{ lbm/s}$ .

### 3 Customer Requirements

#### 3.1 Background

The primary customer of this project was Anthony Linn, who is a professor within Boston University's mechanical engineering department. Professor Linn is an instructor for aerospace-related courses, such as ME425, which involves topics relating to compressible flow and propulsion. The main request was to design a gas turbine system using an automotive turbocharger for the purpose of classroom demonstration of compressible flow principles. As the project progressed, Professor Frank DiBella became a secondary customer. He requested the inclusion of a generator for power generation and assisting with system start-up.

### 3.2 Key Findings

The team went into the initial customer interview with a list of questions about power output and ideas of equipment that could be powered with a gas turbine. However, through the interview, the team discovered that the customer did not want to power anything with the gas turbine. The customer wanted a way to measure properties at various points in the thermodynamic cycle to support classroom analysis. Eventually, the customer may have students design free turbines to attach to the exhaust of the system. To test different fuels in the future, the combustion chamber had to be replaceable. Therefore, it was necessary to make the gas turbine modular (using flanges).

In order to measure the necessary properties, an instrumentation system needed to be designed using LabVIEW so data could be displayed in real time and recorded. Long recording intervals were not a requirement since the system should reach steady state. Among the properties that were needed to be measured include the following: turbine speed, atmospheric pressure, compressor outlet pressure and temperature, turbine inlet pressure and temperature, and turbine exhaust pressure and temperature.

The system also needed to be mobile and to depend on a portable power supply. The customer wanted the gas turbine, cooling system, power supplies, fuel system, and instrumentation to be configured on a wheeled cart.

The system also needed something that could work as a starter to initiate the entire setup. The customer suggested initially using an air start as the starter system as it would be relatively easy to make and safe to use; however, a motor start was preferred for the future. The customer preferred the combustion chamber to run on a liquid fuel like kerosene, but a dry fuel source such as propane was presented as an acceptable alternative. The customer was not worried about environmental impacts since gas turbines are by design powered by fossil fuels, but the use of metal powder as a fuel was mentioned as a possible future experiment.

To keep the system running after years of use, an oil circulation system was needed for the shaft and bearings. This would require an oil pump and tubing. The system can get very hot, so a water cooling system was preferred, which included a pump, tubing, and a radiator. To increase heat transfer away from the radiator, a fan was a possible necessity.

### 3.3 Engineering Specifications

<u>Subject</u>	<u>Specification</u>
<b>Fuel</b>	Kerosene-based jet fuel (preferred) Propane / “dry fuel” (acceptable)
<b>Power</b>	Portable

	Enough power for all instrumentation, fuel, cooling, oil circulation, and motor systems
<b>Support</b>	Mobile and self-contained (manufacture a carriage)  Tested outside
<b>Material</b>	For Combustor: Outer part made of plain carbon steel (stainless would be preferred for corrosion resistance), inner part made of 400 Series Stainless Steel. (no preference stated, advice given)  For Carriage: metal is required (steel or aluminum)
<b>System Control</b>	Fuel flow feedback (closed loop control) is a possible improvement for the future (prevent overspeed)  Interlocking oil pressure with fuel pressure is a possible improvement (prevent shaft damage)
<b>Instrumentation</b>	LabVIEW system is preferred (real-time data), a laptop located on a carriage, Arduino with a compatible display could be used as an alternative.  USB enabled data recording  Long recording times are not necessary (mostly steady-state)  Necessary transducers: <i>Turbine RPM/speed, atmospheric pressure, compressor outlet pressure and temperature, turbine inlet pressure and temperature, and turbine exhaust pressure and temperature</i>
<b>Size</b>	Should fit in a standard elevator and through a doorway  Provided turbocharger came from a 6.6L diesel engine
<b>Cooling</b>	Water (antifreeze) cooling is a priority to prevent oil coking
<b>Oil System</b>	Oil required (advice is 40 psi, “automotive engine oil pressure”)

## 4 System Design

### 4.1 Early Stage Combustion Chamber and Flame Tube Design

The basis of the combustion chamber was to utilize the chemical potential energy of propane to generate power to the turbine of the turbocharger. For a conventional automotive engine, this process occurs in a cyclic manner with the exhaust gasses coming from each of the piston chambers. However, this method for the purposes of this project is inefficient at purely generating exhaust energy for the turbine since work is being done to turn the crankshaft of an engine. Thus a design taken from the aerospace industry, specifically the annular combustion chamber was used.<sup>6</sup>

One of the most important aspects when it comes to designing a combustion chamber for this type of project was to attain a proper size for the flame tube. In an actual combustion chamber, the flame tube or burner is where the combustion of the air and fuel mixture occurs, and as a result, was crucial to a chamber that would both supply but not blow out the flame with air. Like the actual combustion chambers used in professionally built gas turbines, a key aspect is the presence of liner holes spread throughout the length of the flame tube. Most designs used a uniform distribution as well as a uniform diameter perforations in the flame tube to facilitate adequate air dilution. However, specializing the flame tube into regions in accordance with the development of the expanding gasses along the length of the combustion chamber was a design aspect aimed to improve the efficiency performance of the device as explained in *Section 2.5*.

According to multiple projects surrounding combustion chambers for turbochargers, the diameter of the flame tube has to be roughly twice the diameter of the turbocharger's inducer. Additionally the length of the combustion chamber should be six times the inducer diameter. As mentioned before the liner holes are placed within several zones which are the primary, secondary, and tertiary zones. The primary zones usually contain numerous smaller diameter holes. The secondary and tertiary zone features intermediate sized holes and the largest diameter holes, respectively.

The initial design of the flame tube, serving as the prototypical baseline for subsequent iterations, featured 24 liner holes of 7.16 mm in diameter in the primary zone, 8 liner holes of 10.12 mm in diameter in the secondary zone, and 8 liner holes of 16 mm in diameter in the tertiary zone. The design of the combustion chamber housing needed to permit the air flow from the compressor circulating while mitigating excessive material usage, thus it was dimensioned with greater than a 15mm gap around the flame tube. The inducer diameter of the provided turbocharger was 64 mm. Thus utilizing the design principles mentioned previously, the flame tube was designed with a width of 128 mm in diameter, and a length 384 mm.

---

<sup>6</sup> Al Ameen Hassana, Bavanitha Sivasubramaniamb, Daphne Miriam, Hephzin K Varghese, G. Dinesh Kumar , V. Paulson, "Modeling and Simulation of Combustion Chamber for a Turbocharger Jet Engine", *AIP Publishing*, 2022.

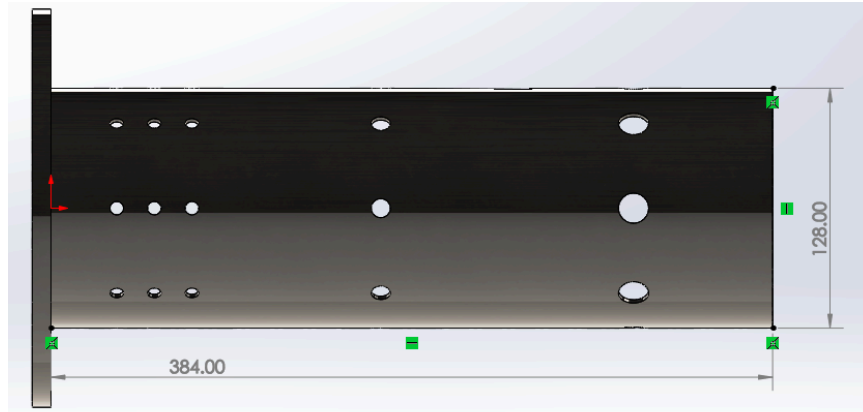


**Figure 10.** The original prototype flame tube design featuring its length and width.

CFD software was used to determine the best design to move forward with. Indicators such as pressure distributions at perpendicular cross-sections along the flame tube would give a better mapping to the introduction of air to properly supply the combustion process.

More revisions were made to the flame tube design including the addition of more holes and varying the sizes of liner holes at each zone. This was done based on the results from the flow simulations which provided a rough idea of how the air circulation may be during the operation of the combustion chamber.

#### 4.2 Late Stage Combustion Chamber and Flame Tube Design

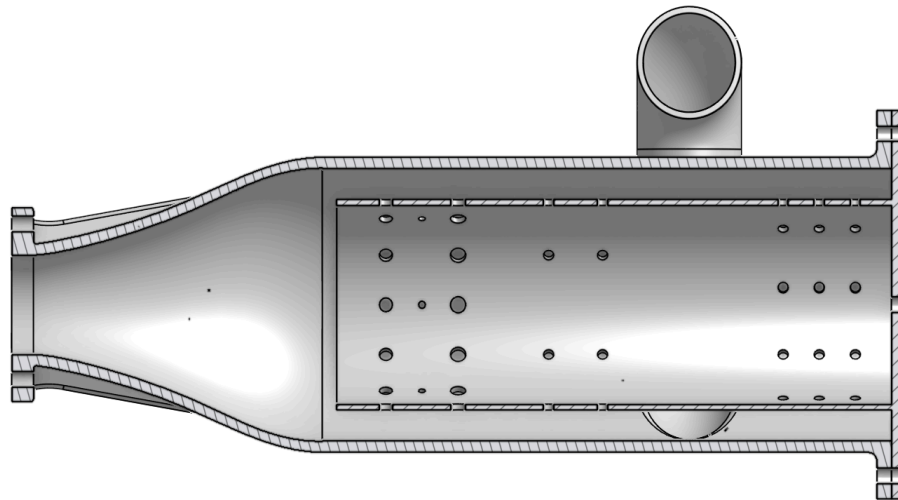


**Figure 11.** Flame Tube Revision 5 Cross Section Inside the Combustion Chamber

Revision 5 of the flame tube design follows the design conception of previous researched designs. The flame tube acts as the rear wall of the combustion chamber and was designed to be easily bolted into the combustion chamber in case the flame tube needed to be changed. The idea

was to design an interchangeable flame tube in the use case of testing multiple designs to evaluate the performance of the device. The inlet pipe from the compressor was also designed off center from the symmetrical midline to prevent conflicting crossflows when the airflow travels around the flame tube. The following table (shown below) shows the hole arrangement of the primary, secondary, and tertiary zones with the total hole area of the flame tube being relative to the area of the inducer of the compressor.

**Table 1.** Configuration of the Primary, Secondary, and Tertiary Holes of 5th Flame Tube Design

Hole Arrangement (per hole)	% of Zone Hole Area	% Total Holes	Total Hole Area (mm <sup>2</sup> )
Zone 1: (27x) 7.0325 mm Zone 2: (12x) 7.071 mm Zone 3: (12x) 10.62 mm (6x) 4.792 mm (12x) 9.079 mm	Zone 1: 69% Zone 2: 31% Zone 3: 89%	189%	6,080.13

Compared to the first flame tube design (in *Section 4.1*), the fifth revision features smaller but more holes in the primary zone. The larger total area of holes (189% to the compressor diameter) was designed to adequately supply air to the propane to meet a 15:1 air/fuel ratio and to encourage more controlled air/fuel micromixing. The tertiary zone features three rows of holes which encourages cooling across a greater length of the flame tube compared to the initial design (from *Section 4.1*). As a result, the design from Figure 10 is the resultant design of the flame tube with a revision in the outer combustion chamber.

### 4.3 Electric Generator in Parallel (Pulley System)

To generate electrical power from the turboshaft a generator would be used. However, due to the characteristics of turbochargers with the speeds, torques, and friction on the shaft, a robust system for reducing the RPM is necessary to prevent the need for designing and fabricating a generator capable of being run one to one with the turboshaft.

#### 4.3.1 Pulley: Generator Assembly Design

Surrounding the specifications of the 10 horsepower induction motor/generator, the maximum rated RPM of the machine is 3600 RPM. From the turbo map of the Garrett GM 19329916 turbocharger, the target RPM was specified to be run at ~70,000 RPM. Thus, a reduction of roughly 19.4:1 was required. Due to the size constraints of the cart, using one pulley would result in a pulley wheel being greater than a foot in diameter which would cause problems

for packaging. A gearbox system would address the packaging issues of a large single pulley system, however, a constant supply of oil as well as no vibration dampening made this option unideal for the purposes of the project. Thus, a dual pulley system was preferred for packaging reasons (seen in Figure 12 below).

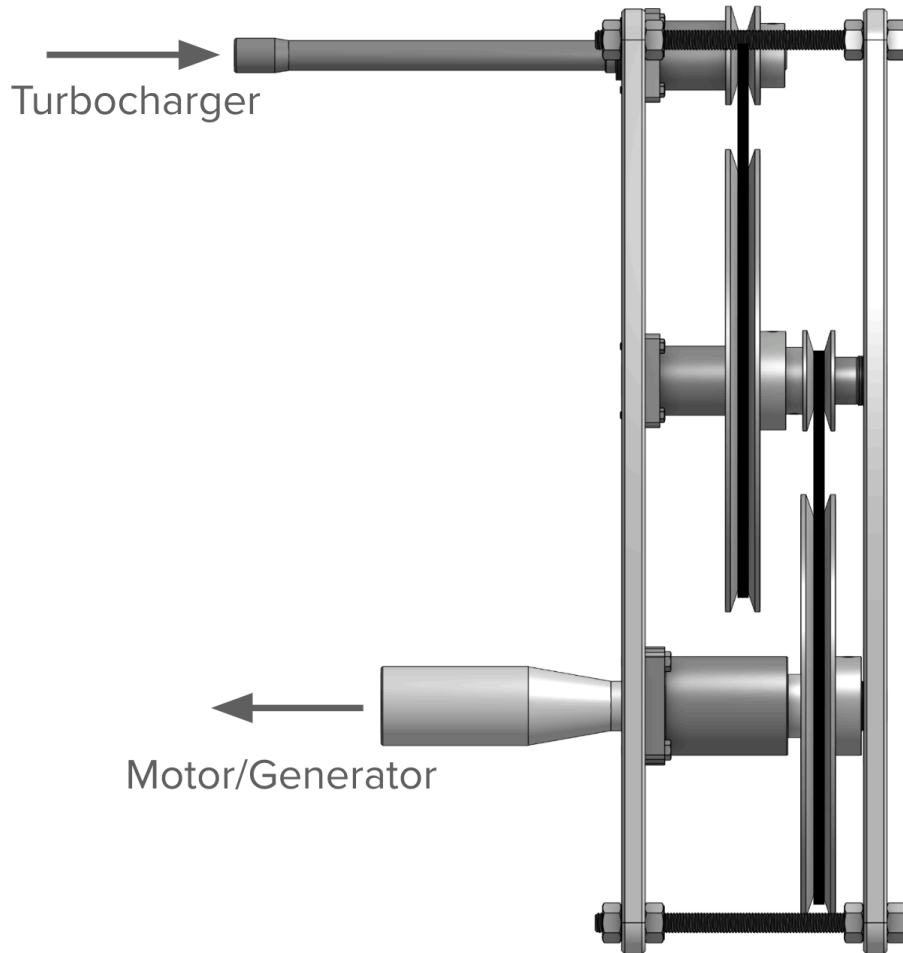


**Figure 12.** Dual motor/generator pulley system with keyed turboshaft and generator shafts

The dual pulleys were designed to be similar in ratio under the pretense that a pulley ratio too large would cause slipping which would affect the efficiency performance of the system to deliver a stable transfer of torque and RPM to the generator. The top pulley was designed with a pulley ratio of roughly 1:4.3 with the bottom ratio being about 1:4.6. This would give a total RPM reduction of 1:19.78 which would run the generator at ~3,488 RPM (lower than the rated maximum 3,600 RPM) to allow for overspeed safety assurance. On the issue of safety, improperly tensioning the V-belts in the pulley may cause the belts to snap when too loose or can cause stress to the bearings and wheels when over tensioned. This can cause unexpected failures leading to injuries for the user caused by improperly specing the wheel ratio being too large. To

address this issue, an analysis into the tensioning of the belt system was conducted with a safety ratio of 5 or below being considered as “safe” for operations.

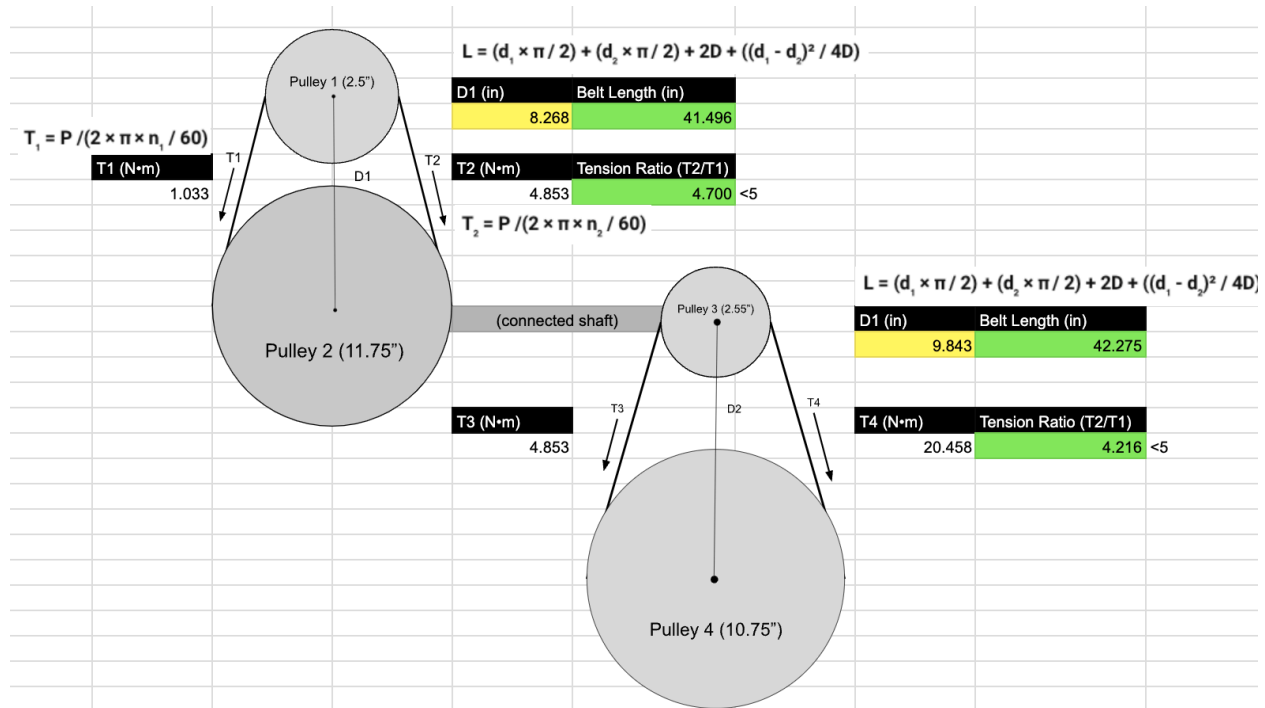


**Figure 13.** Dual pulley safety and belt length analysis of specified assembly

From Figure 13 above, the tension on each side for each the pulley was calculated using the equation:  $T = P / (2\pi \frac{n_x}{60})$  where  $n_x$  is the RPM of the driving shaft and  $P$  is the power of the generator in watts (~7457 watts). As seen above, the tension ratio between the two sides of pulley 1 was calculated to be 4.70 which falls below the safety rating of 5. Likewise, for pulley 2, the tension ratio was found to be lower at 4.216 which also falls below the rated spec of 5. All in all, based on the results of the analysis, the pulley wheel design should be able to run under the sustained loads of the turbocharger powering the generator.

Ceramic flange bearings with self alignment were selected for the purposes of this application as they offer sustained high RPM operations with flange bearings to provide friction relief to constrain the shafts from sliding along its central axis. The entire assembly would be held together between two plates of aluminum metal and threaded rods with a mesh guard to protect users from injury. The shafts are keyed with the generator shaft matching a slotted gap and the turboshaft matching a hex face to ensure a proper transfer of torque to the extended shaft. With regards to the turboshaft, the material was chosen to be carbon steel which matches the same material as the turboshaft itself with a larger diameter of 19.05mm. This will ensure the shafts material endurance under sustained running conditions.

### 4.3.2 Mesh Guard

The pulley assembly was designed to run at very high speeds. With the current design, the internal components such as the pulley wheels and shafts are out in the open without anything to prevent potential situations where accidents might occur. For safety reasons, mesh panels were added to the sides of the pulley assembly, most notably at the parts which are exposed into the open. To do this, two 11 by 12 inch mesh panels were cut and used to block the openings of the pulley assembly. In addition to this, a solid panel was added to the top of the pulley assembly as well that runs along towards the shaft. One thing to note, the top panel can also be replaced with mesh panels for possible weight reduction, The figure below shows how the mesh panels are to be placed.

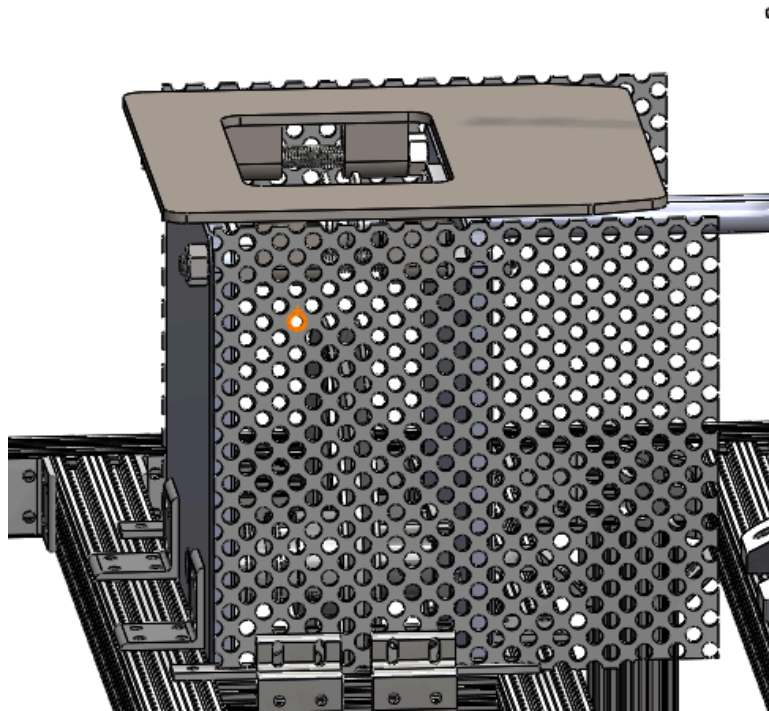


**Figure 14.** The mesh panel setup for the pulley assembly

## 4.4 Carriage/Cart Design

### 4.4.1 Overview

Part of this project involved trying to find a way to make the entire gas turbine transportable. There are a lot of factors that go into the design process behind ensuring the possibility of this to be done. Among these factors include the sizing, materials, attachment points, and cost to make the entire carriage. Sizing is a major aspect to the design process as improper sizing can lead to either the cart becoming too large and unwieldy, or too small and unable to fit every single component onto the carriage. The customer was not too concerned with

the size of the cart design as long as it could fit through a standard 3 feet (914.4 mm) wide door and the elevator within the school's engineering building as well as being self contained.

#### 4.4.2 Initial Design Stage

The design process of the system carriage consisted of multiple stages. In the initial stage, a carriage with an initial length of 60 inches, a width of 36 inches, and a height of 36 inches was made (1524 mm long, 914.4 mm wide, 914.4 mm height respectively). In addition to this a smaller three foot box shaped design was made.

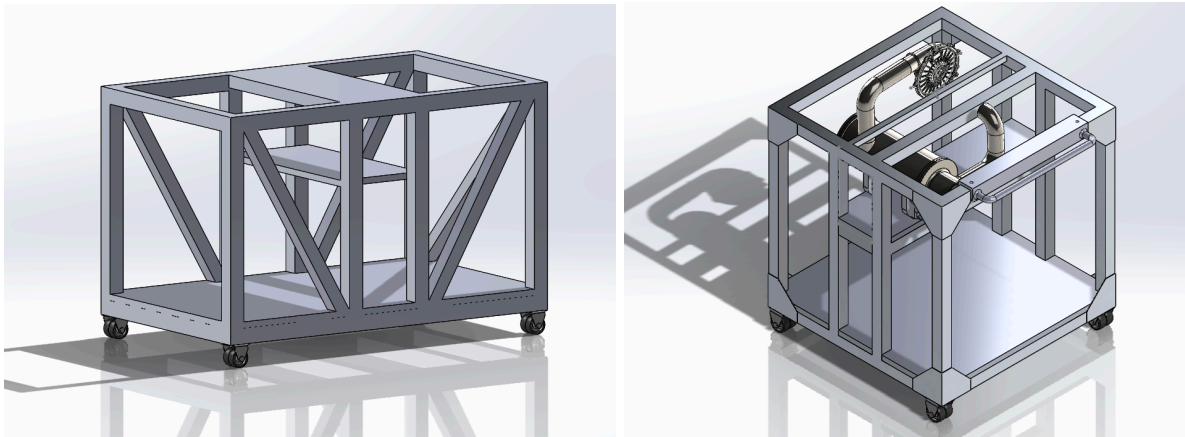


**Figure 15.** Solid models of the 5 x 3 x 3 ft (1524 x 914.4 x 914.4 mm) cart design (left) and 3 ft (914.4 mm) box design (right)

However, after iterating through the design suggestions, the team came to a realization that making the cart three feet wide provided too little of space to actually navigate through a standard three foot door, and also a height of three foot might be too short. Additionally a length of three feet might be too short to properly house the entire setup unless one was to design only for the gas turbine and not fitting anything else ie a propane tank, the system controls etc. Thus a final dimension consisting of a length of 60 inches, width of 33 inches, and 42 inches in height (1524 mm length , 838.2 mm width, 1066.8 mm height) was suggested. The chosen length provides ample space to fit all components into one carriage, thus providing easy transportation of everything. The width would ensure that the cart can both fit through most doors with enough space to turn a corner as well as providing enough width for all components to fit inside. Lastly, the height will make it easier for the user to handle the entire system without having to bend over to adjust the components near the top of the carriage.

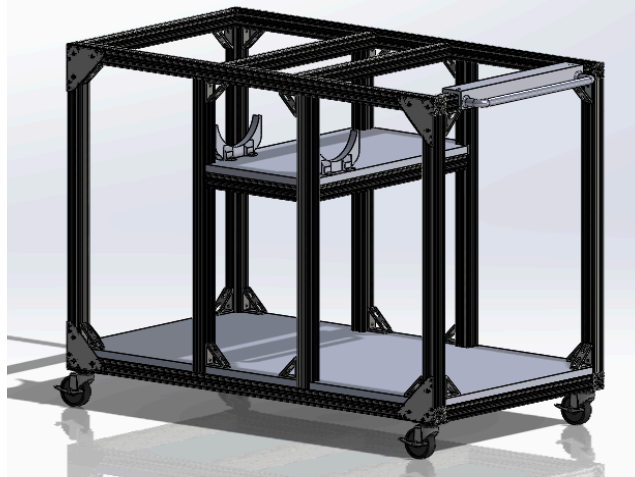


**Figure 16.** The chosen structure made during the initial design stage to which all further designs will be based on.

#### 4.4.3 Later Design Stage

With the chosen dimension and general structure of the carriage chosen, the team then moved on to the next stage of the design process. By this time more components were needed to be considered so overhauls to the general structure were conducted. This involved adding some more supports, most notably at the location of the pulley assembly as well as replacing the larger floor panel with smaller sized parts to save on weight and possibly lower the cost. Additionally the casters originally chosen for the cart were swapped for a different set that can support a higher load as the additional components contribute significantly more weight to the entire system.

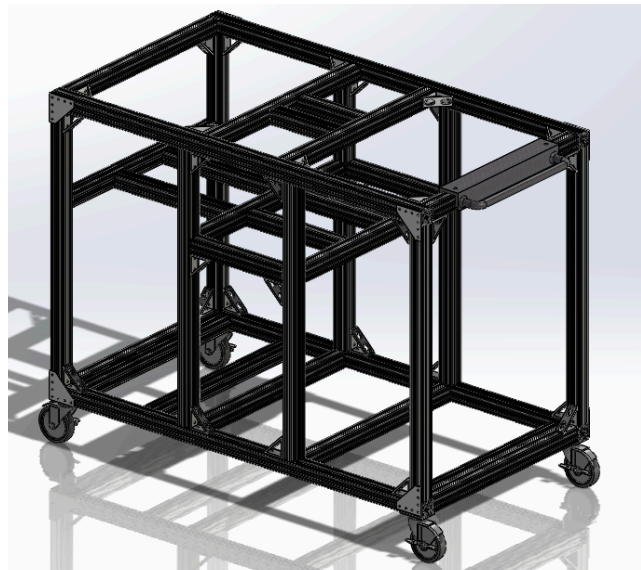


**Figure 17.** The intermediate design, which features more extrusions as supports as well as the removal of the large floor panel.

#### 4.4.4 Final Design

As the project progressed and even more components were added, most notably the finalized pulley assembly and the cooling system (radiator, oil pump, water pump, etc), the cart was once again modified. One notable addition is the addition of another shelf. In the previous designs, the combustion chamber and induction motor were both placed on the same shelf, however with the addition of a flow meter and the need of a check valve, the combustion chamber was moved to a shelf below the original location to accommodate the necessary additional length of the pipe needed for those components. Another addition is additional extrusions placed at the top level of the cart at the location of the pulley. These were added in order to provide further support for the pulley assembly which can be especially heavy. More gussets and brackets were added as well to ensure that the entire cart can withstand all the loads from the combined components .



**Figure 18.** Finalized design featuring more extrusions to allow for better support of the pulley system, as well as a bottom panel to hold various cooling system components.

#### 4.4.5 Materials

As mentioned before another important aspect of the cart design is trying to find the right material for its construction. This also ties into the cost aspect as different types of materials will

have differing costs to purchase. Two likely candidates to be used to make the cart include aluminum and steel. When deciding between the use of steel or aluminum, the main factors were the cost and ease of use. The price of steel ranges between being more cheap than most aluminum such as carbon steels and more expensive with stainless steels. The ease of use was another deciding factor. The group currently has access to aluminum extrusions within the campus and can also potentially order some premade ones that can then be bolted and screwed together. With steel, some more machining might be required as well as potential welding of parts together. The team ultimately decided to move forward with aluminum extrusions as the chosen material to construct the cart. The specific type of aluminum used for the extrusions is 6105-T5 aluminum which provides great strength to withstand the loads that the system components might have on the structure.

The aspect of cost poses a challenge. The current chosen design includes many parts as the entire cart will be constructed out of two inch thick aluminum extrusions as well as other parts like some braces and metal or wooden flat board for the bottom shelf to hold many of the carts components. The extrusions alone will cost a sizable amount as will the necessary supports like gussets, brackets, and necessary t slots fasteners used to attach the extrusions together.

#### **4.4.6 Structural Analysis of the Cart**

In order to confirm whether the structure and material used can withstand all the loads from the components, some analysis had to be performed on the cart design itself. To do this, a model of the cart was made in Solidworks, with the extrusion being represented by two inch hollow beams with an inner dimension of 1.95 inches (a thickness of 0.025 inches). The model itself can be seen in the figure below:

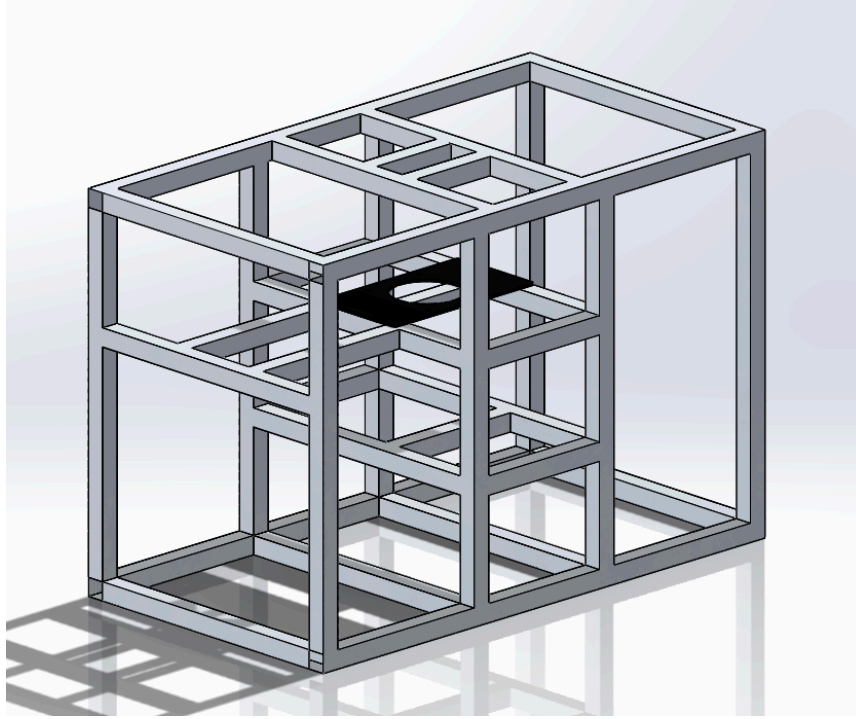


**Figure 19.** Representative model of the cart design used for structural analysis.

After making this model, a finite element analysis was conducted using Solidworks simulation suite. The material chosen for the simulation was 6105 aluminum. The structure was modeled as being fixed to the ground and several forces were applied onto the cart, each being based on the load from the components and located where the components would be situated on the actual cart.

The results from the simulation provided insight on the stresses, strain, and displacements that the cart could undergo once all the components are placed on the structure. From the results, the max stress that the cart could undergo is 30 MPa. The 6105-T5 aluminum used to make the extrusions have a yield strength that ranges from 120-260 MPa. Additionally the fasteners used to attach and support the extrusions have yield strengths of 170,000 ksi which is around 1100+ MPa. This indicates that the structure should be able to withstand the loads. Additionally, this could also indicate that more adjustments can be made such as using smaller 1.5 inch single rail extrusions instead of 2 inch quad rails to create the cart.

The results from the displacement simulations show that the greatest expected displacement is around 0.65 mm located at the location of where the pulley assembly would be placed. In addition the locations of greatest displacement all occur at locations where the heaviest components are situated. Additionally the strain results show a range from  $1.173\text{e-}8$  to  $2.418\text{e-}4$ . Their stress, displacement, and strain plots can be seen in the figures below.

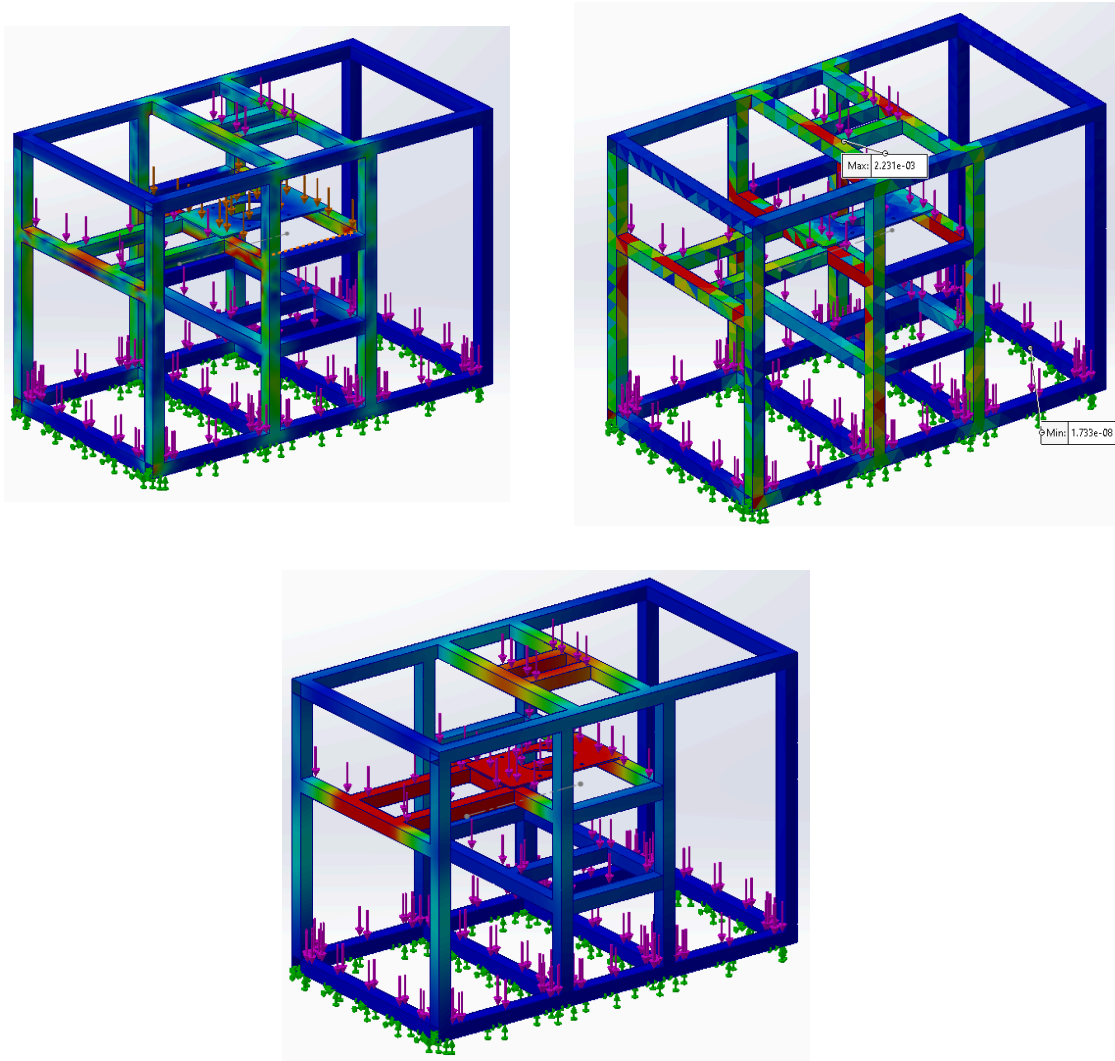


**Figure 20.** The results from the stress, displacement, and strain simulations and the location of the forces applied.

#### 4.5 Mounting Points for the Turbocharger

Another challenge during the design process for the carriage includes the need for proper attachment points. The Garrett turbocharger supplied was for a Duramax LLY engine which has a very distinct style of attachment point for the turbine side in which it features twin inlet pipes oriented perpendicular to the turbocharger. The geometry of the point where it can be secured into place onto the cart from would be another challenge as it was both asymmetrical and featured an unusual curvature.

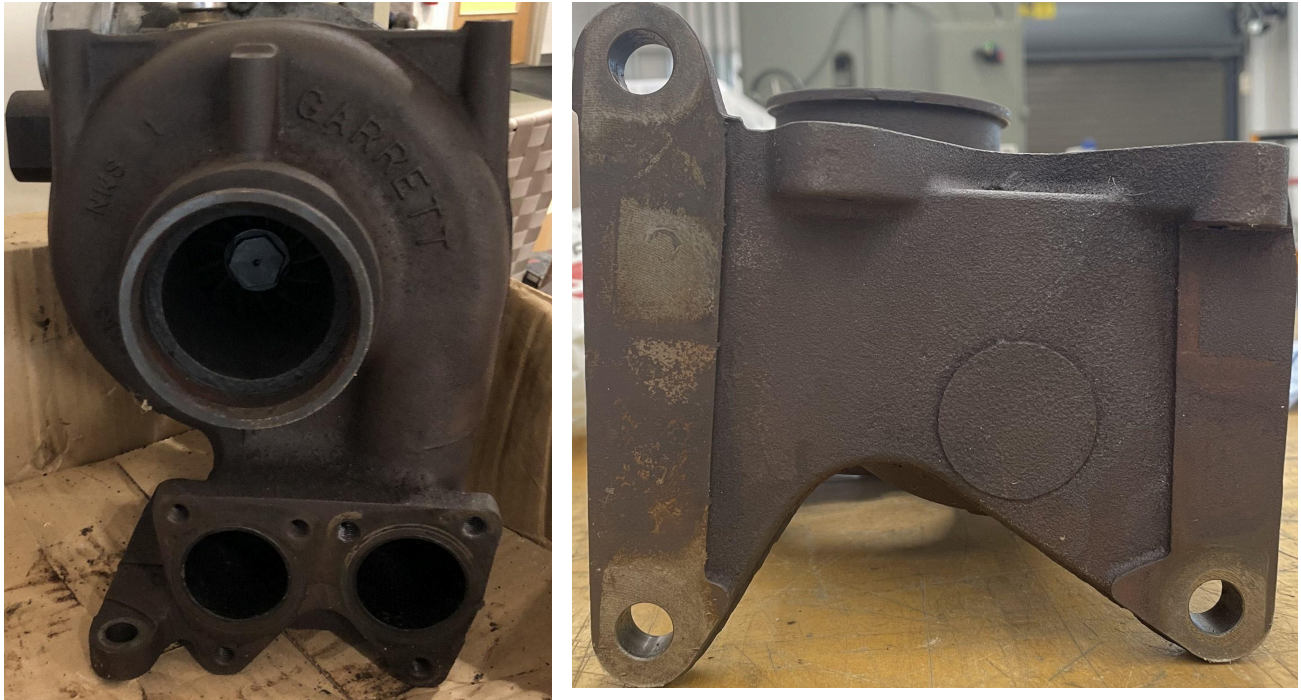


**Figure 21.** The turbine side of the turbocharger featuring the LLY style attachment points near the inlet. The picture on the right showcases the bottom of the turbocharger where the mounting points are located.

The current plan is to orient the turbocharger at the top of the carriage, and to address the unusual shape of the attachment points, a riser was made with a geometry that roughly matches to the one featured on the turbocharger.

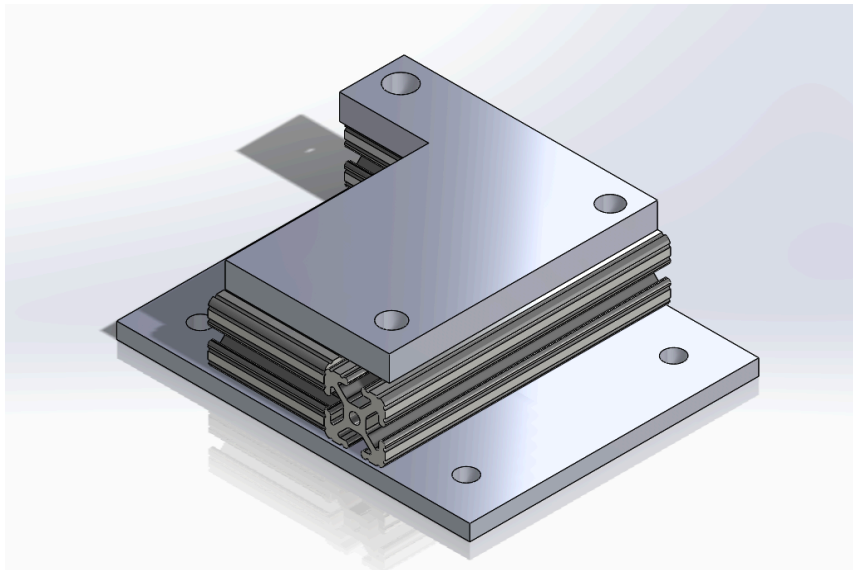


**Figure 22.** Initial design for riser and holder for the turbocharger

The turbocharger's geometry was designed in a way that does not allow it to sit flush on any platform, so the riser was necessary to allow for the desired orientation for the current design of the gas turbine system. The initial design for the riser consists of several 1.5 inch aluminum extrusions cut into multiple lengths to allow for it to conform to the shape of the bottom of the turbocharger's connection point. The dimensions of this specific bottom panel design is roughly 7 inches in width and 8.5 inches in length (177.8 mm width, 215.9 mm length). The chosen material for the panels was steel as it provides enough strength to accommodate for the weight of the turbocharger as well as handle the high temperatures that the turbine may operate at.

A newer design was later devised over the following semester. The main focus behind this newer turbo mount was to both allow for it to better conform to the turbocharger's geometry as well as to allow for a more secure attachment onto the carriage. It consisted of a machined block of 6061 aluminum and has the following dimensions: 12 inches in length, 7 inches in width, and 2.5 inches in depth (304.80 mm length, 177.80 mm width, 63.50 mm depth). The aluminum block will be required to be purchased from vendors in the form of aluminum stock that is cut into a dimension of 12 x 7 x 3.5 inches. Several holes will need to be machined as well to account for the attachment points. Since the cart is made from 2 inch quad rail aluminum extrusions,  $\frac{1}{4}$ -20 screws will be needed. The location where the mount attaches to the cart is near the front of the mount and along the sides. Hence the hole diameter will need to be  $\frac{1}{4}$ " as well to accommodate for this. Additional holes that match the turbocharger will also need to be machined near the rear side of the mount.

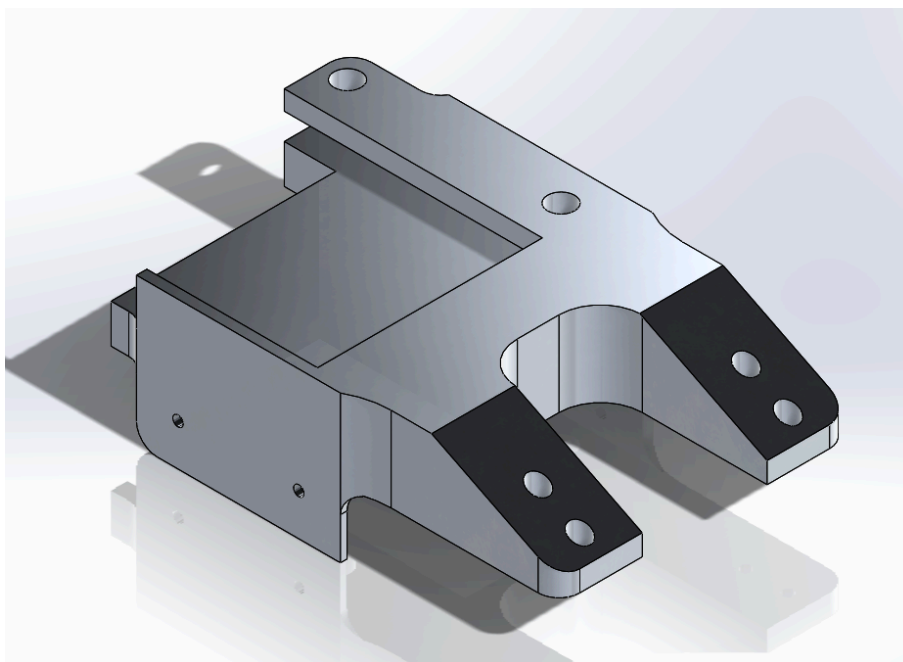


**Figure 23.** Final design for riser and holder for the turbocharger

With the design finalized, it's also important to acknowledge some potential issues. One of the main issues is the overall complexity of the part. It will have to be machined and the geometry of this mount can pose a challenge to recreate. Additionally the size of the block

needed can be very expensive (>\$229). Aluminum 6061 was chosen as the material since it's lighter than steel, but another issue arises when taking into consideration the turbine's operating temperature which can reach as high as 1050 degrees fahrenheit. The melting point of 6061 is around 1081 degrees F and is very close to the aforementioned operating temperature. Possible solutions to this might be to add insulation at where the turbocharger attaches onto the mount.

#### 4.6 Pipe Configuration

In order to allow the flow of air to move from the compressor to the combustion chamber and from the combustion chamber to the turbine, a set of pipes would be needed. The pipes used for this system are made from 304 steel tubes with an outer diameter of 2.5 inches and an inner diameter of 2.37 inches. This results with a wall thickness of 0.065 inches. The tubes will be cut into sections and have plates with  $\frac{1}{4}$ " holes welded at the ends. Alternatively the tubes would be welded onto each other to complete the connection.

The need to break them into sections comes from the fact that a check valve and flow sensor were both needed for the system. Additionally corner elbow tubes were also sourced to create the necessary bends used in the pipe design. In addition to the check valve and flow sensor, pressure and temperature transducers were also placed throughout the pipes at various locations for the sake of sensing the characteristics of the air flow at both the compressor stage and turbine stage. There is also a presence of an intersection opening near the entrance of the combustion chamber to allow for the compressed air from the air starter to help kickstart the system. The figure below provides a look at both the finalized pipe for the compressor and turbine sides.

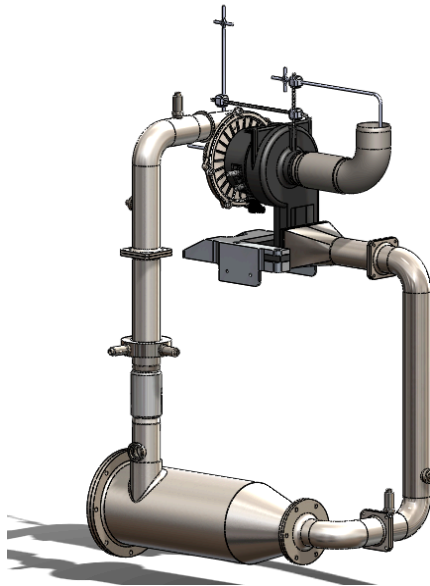


**Figure 24:** Finalized pipe setup for both the compressor side (left) and turbine side (right)

#### 4.7 Final Gas Turbine System

With the cart structure finalized and the rest of the system components accounted for, the entire gas turbine system was then assembled. There are many elements to the entire system as a whole, but the major components are turbocharger, combustion chamber, the pulley assembly, the induction motor, and propane tanks. All the components aside from the air starter were packaged within the cart, thus achieving the self contained aspect of the entire system. Additionally the casters can allow for the entire system to be moved to a new location without the need for an external source of transportation. A final render of the gas turbine system can be seen in the figure below.

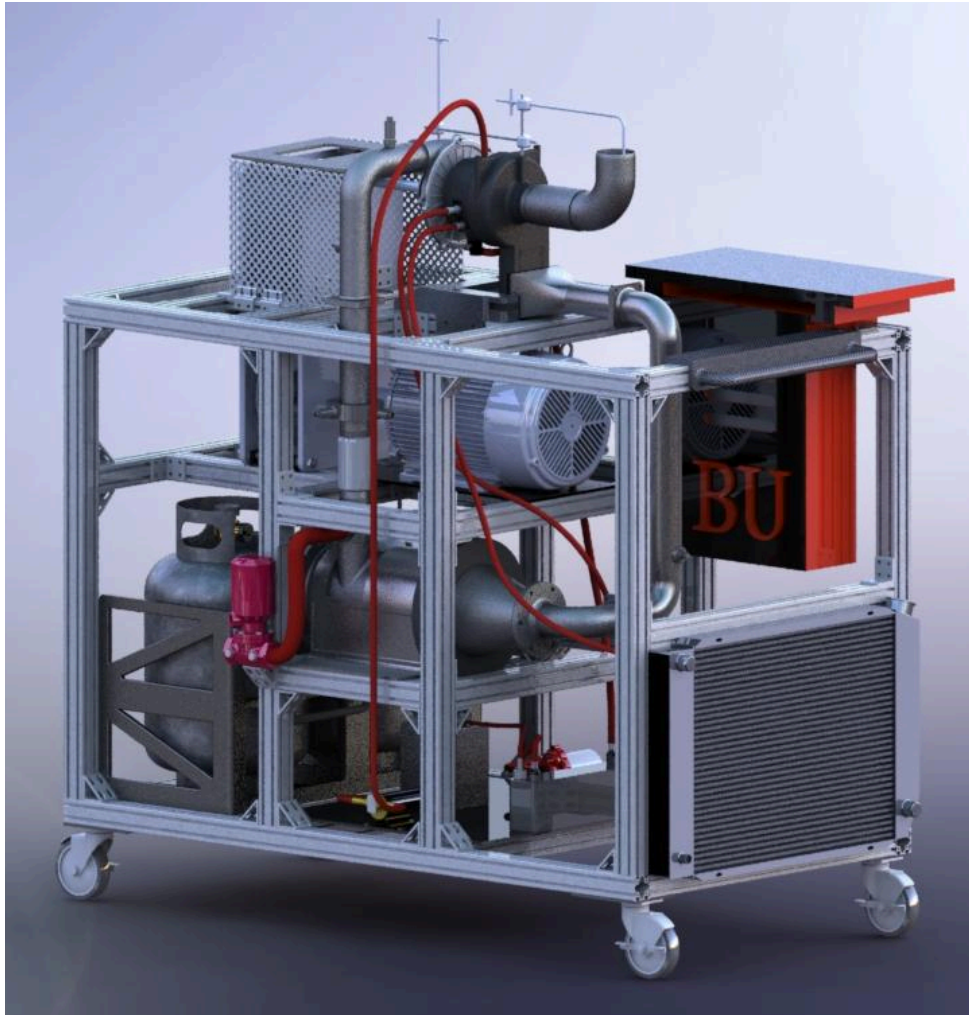


**Figure 25.** The finalized gas turbine system.

## 4.8 Electrical System

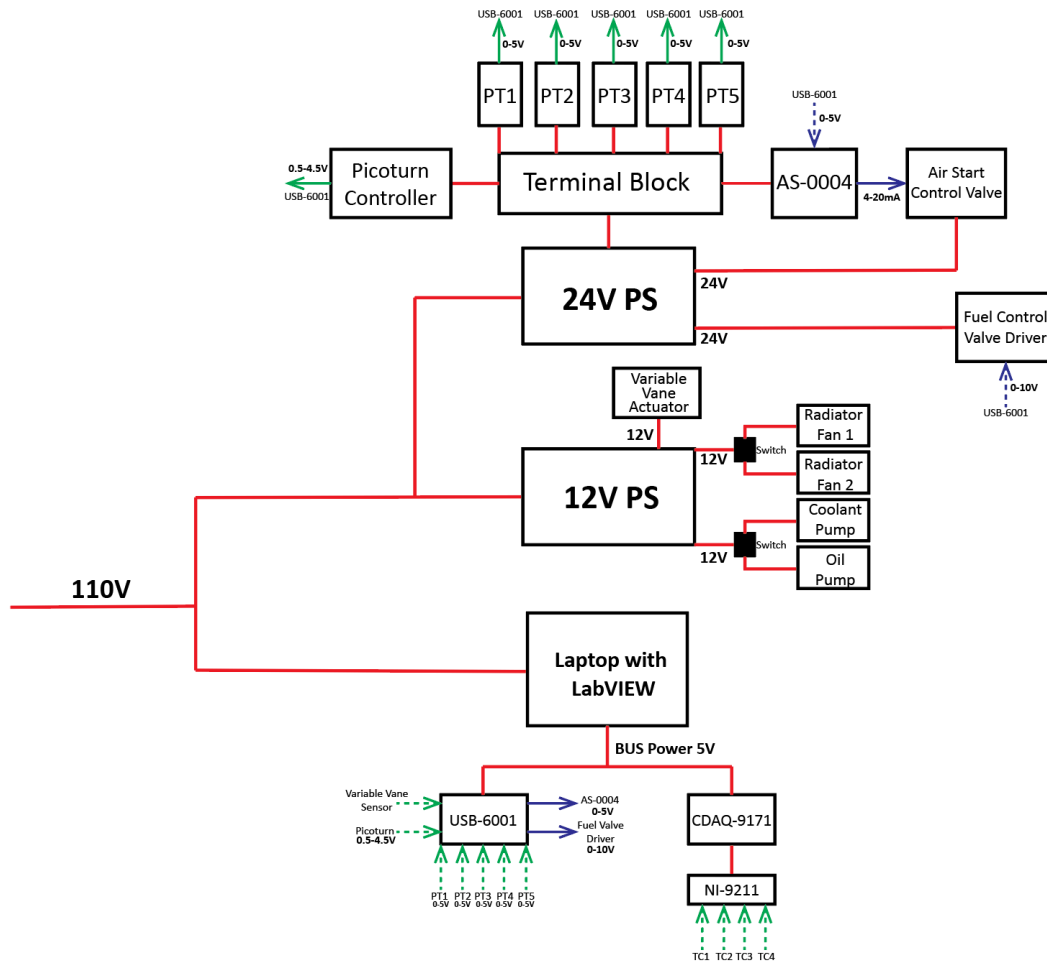


**Figure 26.** Full electrical block diagram

Figure 26 shows the general electrical system design for the gas turbine system. To ensure a constant power source over the course of the intended lab experiment, the system was designed to run off a 110/120V wall power outlet. Although the system is run outside, an extension cord could be run from the nearest building to a surge protector for power distribution. Two AC to DC power supplies were used (one 12V and one 24V) to power the system components. Separate power supplies were required because a single power supply with 12V output, 24V output, and the 500W required could not be easily or cheaply sourced.

The 24V, 240W supply powers the five pressure transducers, the controller for the Picoturn rotational speed sensor, the driver for the fuel control valve, the air start valve, and the module that converts a 0-5V signal into the 4-20mA required to control the air start valve. The 12V, 600W supply powers the two radiator fans, the two pumps, and the actuator for the variable vanes within the turbocharger.

A laptop was included to run the LabVIEW program that receives measurements from the instrumentation. This laptop powers the two DAQ modules through USB BUS power.

Item	Links	Voltage Possible (V)	Voltage Used (V)	Current (A)	Power (W)	QTY	Total Power (W)	Notes
Pres. Transducer	<a href="https://www">https://www</a>	9-30V	24	0.01	0.24	5	1.2	
Fuel Valve	<a href="https://www">https://www</a>	-	-	-	-	-	-	
Fuel valve driver	<a href="https://www">https://www</a>	24	24	0.5	12	1	12	
DAQ	<a href="https://www">https://www</a>	-	-	-	-	-	-	Powered by computer USB
Chassis	<a href="https://www">https://www</a>	-	-	-	-	-	-	Plugged into chassis
Therm. DAQ	<a href="https://www">https://www</a>	-	-	-	-	-	-	Powered by computer USB
Radiator Fan	<a href="https://www">https://www</a>	12	12	6.67	80	2	160	2 fans, 12V, 80W each
Coolant Pump	<a href="https://www">https://www</a>	12	12	6.74	80.88	1	80.88	
Motor Starter	<a href="https://www">https://www</a>	-	-	-	-	-	-	<b>Needs 240V outlet</b>
Compressed air, voltage to current	<a href="https://www">https://www</a>	7-30V	24	0.02	0.48	1	0.48	
Oil Pump	<a href="https://www">https://www</a>	12	12	10	120	1	120	This is max current, average is 7A
Picoturn Controller	<a href="https://www">https://www</a>	7-30V	24	0.08	1.92	1	1.92	<a href="https://www.mouser.com/datasheet/2/588/AM">https://www.mouser.com/datasheet/2/588/AM</a>
Air Start Control Valve	<a href="https://kim">https://kim</a>	10-30V	24	0.6	14.4	1	14.4	
<b>Grand Total Power</b>							510.88 W	

**Figure 27.** Electrical power analysis for all required electrical components

Figure 27 shows the electrical power analysis that was performed to determine the number of power supplies that were needed to run the system. In addition, the motor starter that was required to safely stop the motor needed a 240V outlet and extension cord to run.

#### 4.8.1 Instrumentation

The customer required that the instrumentation system allowed for real-time data collection through a USB connection. Due to this constraint, the choice for digital data collection came down to either Arduino or LabVIEW: both of which are used extensively in the mechanical engineering curriculum at Boston University.

The initial priority in brainstorming the instrumentation system was low cost. The lowest cost option for data acquisition was an Arduino board (UNO or Mega). This method required either writing sensor data to an SD card using Arduino SD libraries (which was not preferred by the customer) or printing data strings to the Arduino serial monitor and parsing those strings using an Excel macro designed to read serial port data, like PLX-DAQ, or an open-source Python script. An Arduino Mega would have enough analog pins to read data from each of the required sensors (which tend to output 0-5V), but the 10-bit resolution of the Arduino became an issue when choosing a way to measure temperature at each of the required positions. Due to the high temperatures involved in this project, K-type thermocouples (which have a range of -326 to 2300°F) were needed for temperature measurements. Thermocouples output voltages in the

millivolt range, so, without an amplifier, an Arduino would not be able to record useful temperature data. That was coupled with the fact that thermocouples require conditioning to compensate for the cold-junction temperature: an effect of the physical contact between the metal used to sense the temperature and the copper wire carrying the voltage to the measuring device (shown by  $T_{ref}$  in Figure 28)

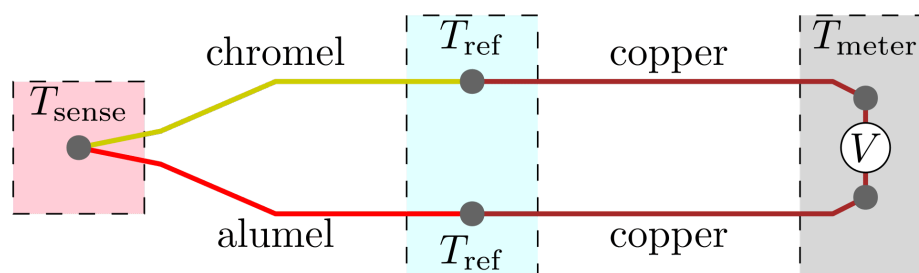


**Figure 28.** Diagram of a K-type thermocouple showing the cold-junction between the copper and chromel/alumel wires

While the low-cost nature of the Arduino solution was attractive, it added complexity through the addition of amplifiers for the thermocouples, and limited the accuracy of any analysis done on the system due to the lower resolution of the Arduino.

The second option for a data acquisition system was to use National Instruments USB DAQ devices, which provided higher ADC resolution than Arduinos. These devices were compact and were powered directly by the computer through USB. The cheapest of those options, the USB-6001, had 14-bit resolution, which allowed for better measurements. NI also had DAQs made specifically for temperature measurement from a thermocouple, and they could be attached to a USB chassis for data transfer. Programs could be easily written in LabVIEW to collect data from these devices, which was beneficial because it gave students more experience with operating LabVIEW. Although NI devices are expensive, they were a worthwhile investment since they allowed for convenient temperature measurements and guaranteed more accurate sensor measurements, which was necessary for a lab demonstration used to teach practical knowledge.

Along with choosing sensors that could provide measurements in the necessary ranges at each station in the cycle, the type of measurement taken and the method of attaching sensors to the system were large parts of the design. Figure 29 shows a cartoon version of the system with the station numbers that will be used for the rest of the report.

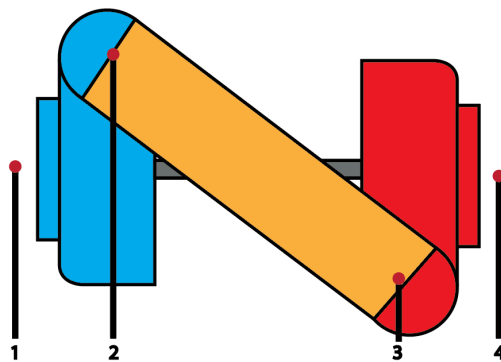


**Figure 29.** Cartoon of gas turbine system with compressor (blue, 1-2), combustion chamber (orange, 2-3), and turbine (red, 3-4)

At the inlet to the compressor (Station 1), conditions can be assumed to be atmospheric, but temperature and pressure sensors were included to meet customer requirements. For temperature measurements, an exposed K-type thermocouple was used. It measures static temperature since the low velocity at the inlet is not high enough to affect the total temperature. A pressure transducer (that outputs 0 to 5 Volts) connected to a pitot-static tube was used for pressure measurements so either static or total pressure can be measured. It was mounted in front of the compressor inlet.

At the inlet and outlet to the combustion chamber (Stations 2 and 3), two ideas were put forward for temperature measurements: surface-mount thermocouples and thermocouple probes with M12 connectors. The benefit of the surface-mount configuration was that there would be no disturbance of the flow from a probe and installation would be simpler. The main challenge with surface-mount thermocouples was the error that would come with the measurement if the sensor was not insulated from ambient conditions. The price of surface mount thermocouples also increased drastically for the temperature at Station 4 (1250°F). Thermocouple probes, on the other hand, benefitted from direct contact with the process fluid, so they measured total temperature without any need for correction from heat transfer analysis. Ultimately, thermocouples with 2 inch probes were included in the system design, and they were attached to the air pipes using ½-inch NPT weld-on bungs.

For the pressure measurements at Stations 2 and 3, stainless steel pressure transducers that output 0 to 5 Volts were used. They were attached to the piping at each station with ¼-inch NPT weld-on bungs. In addition, the transducer at Station 3 would need to be thermally isolated from the process fluid since the max temperature rating on the chosen transducers was 185°F. This could be achieved using specially designed thermal isolators with fins for increased heat rejection. These transducers would measure static pressure.

At the exit to the turbine (Station 4), the same exposed thermocouple set up that was used for Station 1 was used to measure the exhaust temperature, which would be a value between static and total temperature that would have to be corrected to calculate the correct expected

power output. Like Station 1, a pitot-static tube was set up in the path of the exhaust to measure either the static or total pressure using a pressure transducer that outputs 0 to 5 Volts.

In addition to the state values at each station, measurement of the rotational speed of the turbocharger was a customer requirement. The easiest way to measure the speed was to use a compressor wheel speed sensor sold directly by Garrett, as shown in Figure 30.

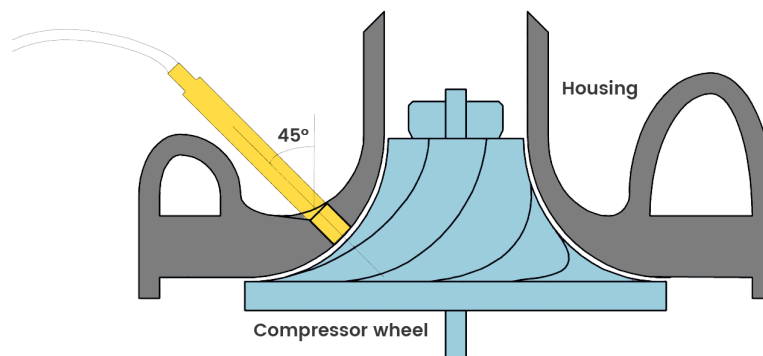


**Figure 30.** Ideal installation of the turbocharger speed sensor into the compressor housing

The issue with this choice was that the Garrett GT3788VA used in the project does not include a pre-drilled port for sensor installation. The team would be forced to drill a hole in the housing to install the sensor, which was not ideal, but it was the best option for directly measuring the rotational speed.

Air flow rate was an additional measurement that was preferred for better system analysis. An orifice plate flow meter was selected for ease of installation since they are designed to fit into large pipe diameters using standard flanges. The meter functions by forcing flow through an orifice and measuring the pressure drop using  $\frac{1}{4}$ -inch NPT pressure transducers. The resolution provided by the transducers allowed for reliable flow rate measurements. The orifice flow meter required a straight pipe length of 5 diameters upstream (12.5 inches for a 2.5 inch pipe diameter) and 2 diameters downstream (5 inches). This created a minimum length constraint for the pipe carrying air from the compressor to the combustion chamber.

#### 4.8.2 Controls and Safety Measures

Once the instrumentation system was in place, the next step was to develop system controls. The most important control for this system was fuel flow control since the fuel flow rate determines the amount of heat added by the combustion chamber, which changes the amount of power generated by the system. The basic idea was to have an electronically controlled valve that could open proportionally to a voltage provided by the output of the USB-6001 DAQ. This could be done using either a solenoid valve with a driver that simulates a PWM signal or with a motorized needle valve. The needle valve was preferred since it would allow for a greater amount of control over the flow. For this fuel control system, the driver would be purchased along with the valve, which allowed for a 0-10V control signal to be provided by the USB-6001

DAQ. The driver required 24V power to run, which was supplied by the 24V power supply included in the electrical box. The basic idea behind the closed loop control was that the position of the needle valve would be controlled by the temperature of the combustor exhaust and would close significantly if the temperature at the exit of the combustor exceeded the design temperature of 1250°F. The flow rate could also be linked to the speed of the compressor in order to prevent overspeed. The needle valve allowed for both precise control and the ability to completely shut down the system by shutting off fuel flow.

The USB-6001 DAQ was also used to control the air start electronic control valve. Instead of requiring a voltage control signal, this valve (Kimray MXC, as described in *Section 4.10*) required a 4-20mA signal to open. Since the DAQ only had a voltage output, a device was required (AS-0004 in the BOM) to convert a 0-5V signal into a 4-20mA signal.

Other important control systems involved oil pressure regulation and the control of the turbocharger variable vanes. Oil pressure could be controlled by using a 40 psi pressure regulator, which would connect to the oil lines and ensure that the pressure within the oil loop remains close to 40 psia. This pressure was required to float the turbocharger journal bearing and to prevent leaks within the turbocharger. Using an off-the-shelf oil regulator saved the team the trouble of designing an electronic control system for oil pressure. The variable vanes were controlled by a 12V solenoid that moves the unison ring on which all the vanes are located. This could be achieved by controlling a MOSFET connected to the 12V battery with the USB-6001 DAQ output signal. As the USB-6001 only allows for two analog output signals, a different device would need to be included to control the variable vanes. This improvement would allow for a change in flow rate once the system was steadily operating.

Safe start-up and maintenance of the entire system was a priority for the team. To ensure the system does not overheat, start-up begins by turning on the radiator fans and the oil and coolant pumps. The two pumps and two fans are connected to two separate relays. To prevent injury, the switches could be controlled from a distance using Bluetooth relays. After running the oil and water lines for a few minutes, the electronic control valve attached to the air compressor would be opened using the LabVIEW algorithm tied to the transient analysis to start the airflow through the system. After two seconds of airflow, the fuel flow valve would be opened using its LabVIEW algorithm. A second later, the spark plug would be fired (an Arduino circuit and Bluetooth module could be used to remotely control the firing. After the system becomes self-sustaining, the air starter control valve would be shut. This start-up sequence would prevent damage to the system and to the students operating it. The system could then be turned off safely by remotely closing the fuel valve and then remotely turning off the pumps and fans.

## 4.9 Cooling System

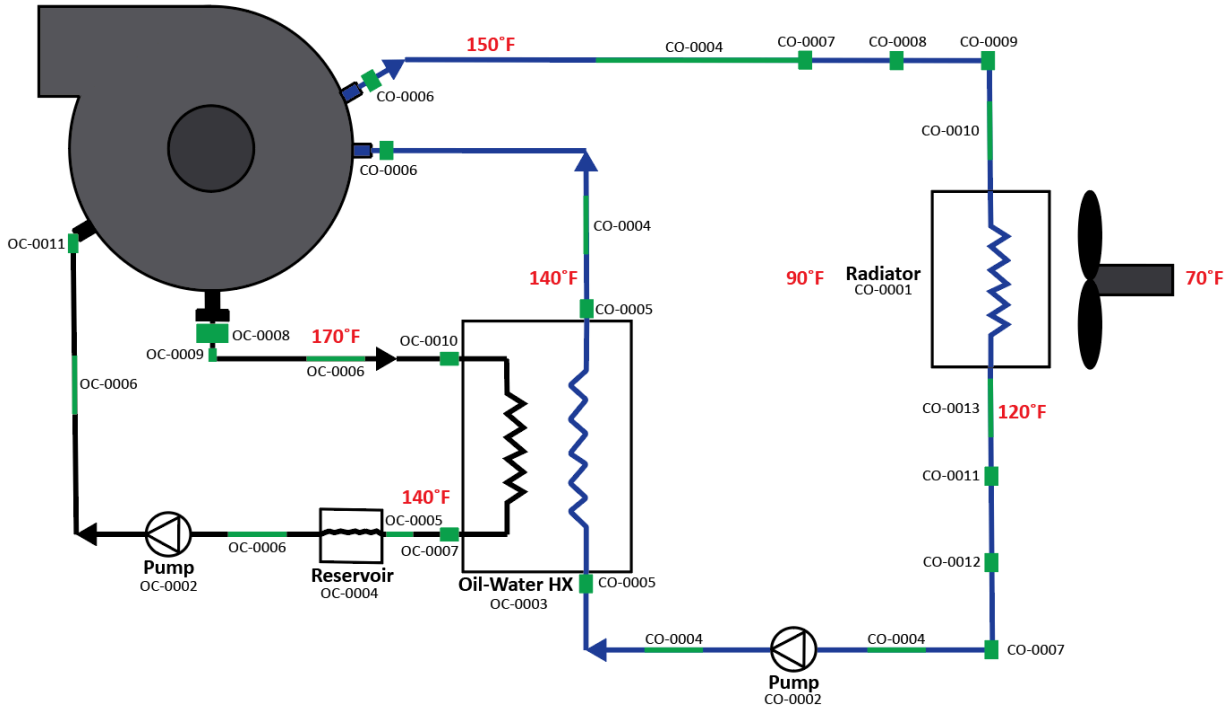


**Figure 31.** Line diagram of the general cooling system

Oil lubrication was a requirement for this system since the turbocharger is spinning at upwards of 70,000 RPM and is supported by a journal bearing that would be damaged without oil. The customer suggested that a water cooling system be used to prevent oil coking, which would lead to damage in the bearing. To meet this requirement, a system with an oil-water heat exchanger and a water-air radiator was developed. Since the turbocharger included a built-in water line, the system water line was hooked up to the turbocharger for further cooling within the housing. All of the part numbers shown in Figure 31 can be found in the BOM.

The cooling system design started with a simple heat balance (Equation 7) for the oil-water exchanger

$$\dot{Q} = \dot{m}c_p(T_{in} - T_{out}) \quad (7)$$

All heat was assumed to transfer from one liquid to the other with no loss to the surroundings.

The mass flow rate of the oil was assumed using a velocity of  $5 \frac{m}{s}$  and an inner diameter of 0.5 inches. The mass flow rate was then calculated using the following formula

$$\dot{m} = \rho V \left( \frac{\pi}{4} D^2 \right) \quad (8)$$

where  $D$  is the inner diameter. The density of the oil was found to be  $53.91 \frac{lbm}{ft^3}$ . The oil mass flow rate was calculated to be  $0.37 \frac{lbm}{s}$ .  $c_p$  was found using the specific heat capacity of SAE30

oil ( $0.549 \frac{\text{Btu}}{\text{lbm R}}$ ). The heat was then calculated using Equation 7 and the inlet and outlet temperatures shown in Table 2. The coolant mass flow rate was calculated assuming a  $c_p$  of  $0.998 \frac{\text{Btu}}{\text{lbm R}}$ , and the volume flow rate was calculated assuming a density of  $62.3 \frac{\text{lbm}}{\text{ft}^3}$ .

**Table 2.** Flow rates for oil and coolant loops and oil-water inlet and outlet temperatures

	Oil	Coolant
Mass Flow	0.37 lbm/s	0.30 lbm/s
Volume Flow	11.6 lpm (3 gpm)	8.27 lpm (2 gpm)
Inlet Temperature	170 °F	120 °F
Outlet Temperature	140 °F	140 °F

The temperatures in Table 2 were all chosen to stay below boiling and coking points for the oil and coolant. With the volume flow rate evaluated for the pumps, pumps were selected for both the oil and coolant to match the required flow rates.

With the oil and coolant temperatures and flow rates defined, the required heat exchanger area was found using the NTU-Effectiveness method. To maximize heat transfer, the design was constrained to counterflow arrangements for the liquid-liquid heat exchanger. The effectiveness of the oil-water heat transfer was determined using Equation 9

$$\epsilon = \frac{q}{q_{max}} \quad (9)$$

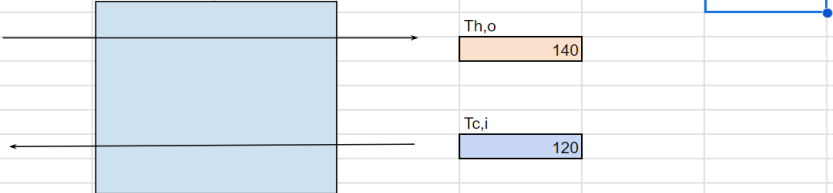
where  $q$  is the actual heat transfer and  $q_{max}$  is the theoretical heat transfer if the outlet temperature of oil equals the inlet temperature of the coolant. For this heat exchanger, the effectiveness was 0.6. The NTU value was then found using the NTU relation for counterflow (Equation 10)

$$NTU = \frac{1}{C_r - 1} \ln\left(\frac{\epsilon - 1}{\epsilon C_r - 1}\right) \quad (10)$$

where  $C_r$  is equal to  $\frac{C_{min}}{C_{max}}$  and  $C = \dot{m}c_p$ . The value of NTU is also equal to the value given by Equation 11

$$NTU = \frac{UA}{C_{min}} \quad (11)$$

where  $U$  is the heat transfer coefficient, which was assumed to be  $100 \frac{\text{Btu}}{\text{hr ft}^2 \text{ R}}$ . This estimate was conservative for liquid-liquid heat transfer since oversizing the heat exchanger was better than possibly undersizing it. Rearranging Equation 11 and solving for the area  $A$ , the required heat transfer area was determined to be  $8.8 \text{ ft}^2$ . Figure 32 shows the spreadsheet that was used to calculate every value that led to the selection of the oil-water heat exchanger (plate heat exchanger,  $0.92 \text{ m}^2$  heat exchange area).

	OIL-WATER								
HX Type	Plate								
Th,i	<div>170</div>			Th,o	<div>140</div>				
Tc,o	<div>140</div>		Tc,i	<div>120</div>					
OIL	values	units	WATER	values	units	HT Parameters	values	units	
v =	<div>5</div>	ft/s	v =	<div>3.57</div>	ft/s	U =	<div>100</div>	Btu/(hr*ft^2*R)	
ID =	<div>0.5</div>	in	ID =	<div>0.5</div>	in	Cmin =	<div>0.202</div>	Btu/R*s	
A,pipe =	<div>0.0014</div>	ft^2	A,pipe =	<div>0.0014</div>	ft^2	Cr =	<div>0.667</div>	-	
Vol flow =	<div>0.00682</div>	ft^3/s	Vol flow =	<div>0.00487</div>	ft^3/s	A,required =	<div>8.8</div>	ft^2	0.8
rho =	<div>53.91</div>	lb/ft^3	rho =	<div>62.3</div>	lb/ft^3	effectiveness =	<div>0.6</div>		m^2
m, dot =	<div>0.37</div>	lb/s	m, dot =	<div>0.30</div>	lb/s	NTU =	<div>1.216</div>		
cp =	<div>0.549</div>	Btu/lb*R	cp =	<div>0.998</div>	Btu/lb*R	*counterflow			
C =	<div>0.202</div>	Btu/R*s	C =	<div>0.303</div>	Btu/R*s	cmax mixed, cmi	<div>1.45</div>		
Q, dot =	<div>6.05</div>	Btu/s	Q, dot =	<div>6.05</div>	Btu/s	cmin mixed, cma	<div>1.42</div>		
	<div>21794</div>	Btu/hr		<div>21794</div>	Btu/hr				
	<div>8.56</div>	hp							
Vol flow =	<div>11.58</div>	lpm	Vol flow =	<div>8.27</div>	lpm				
	<div>3</div>	gpm		<div>2</div>	gpm				

**Figure 32.** Oil-water heat exchanger spreadsheet calculations

After finding the area required for the liquid-liquid heat exchanger, the radiator area and flow rates needed to be calculated. Table 3 shows the flow rates from a heat balance using Equation 8 and defined temperatures (assuming a 70 °F day).

**Table 3.** Flow rates for coolant and air and radiator inlet and outlet temperatures

	Coolant	Air
Mass Flow	0.30 lbm/s	1.89 lbm/s
Volume Flow	8.27 lpm (2 gpm)	42913 lpm (1515 cfm)
Inlet Temperature	150 °F	70 °F
Outlet Temperature	120 °F	90 °F

The same NTU-Effectiveness analysis as above was carried out to size the radiator. Since a radiator can be modeled as a crossflow heat exchanger (coolant unmixed and air mixed), Equation 12 was used

$$NTU = -\ln\left[1 + \frac{1}{C_r} \ln(1 - \epsilon C_r)\right] \quad (12)$$

The heat transfer coefficient  $U$  was assumed to be  $50 \frac{\text{Btu}}{\text{hr ft}^2 \text{R}}$ . Figure 33 shows the spreadsheet used to carry out the NTU analysis for the radiator. A heat exchange area of 12.3 ft<sup>2</sup>



The overall system design involved sourcing a packaged and portable compressor and tank which would then be fed into the combustor through a control valve. The air was routed into the combustor to spin the turbine. Transient analysis of a 30 gallon compressed air tank pressurized to 80 psia yielded the results given in Figure 35. This analysis provided the proof that a control valve was necessary to successfully control the flow rate ( $1.34 \frac{ft^3}{s}$ ) of the system and allow compressed air to flow for an extended period of time.

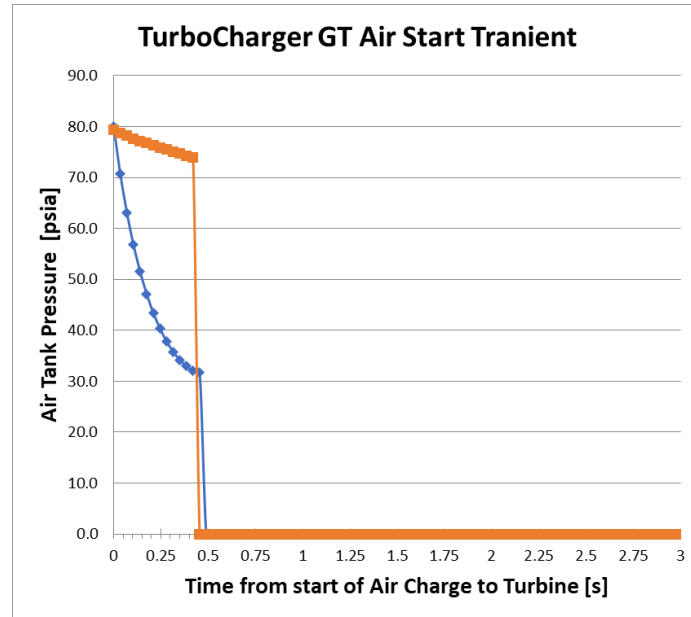


**Figure 35.** Air start transient analysis with (orange line) and without (blue line) a control valve

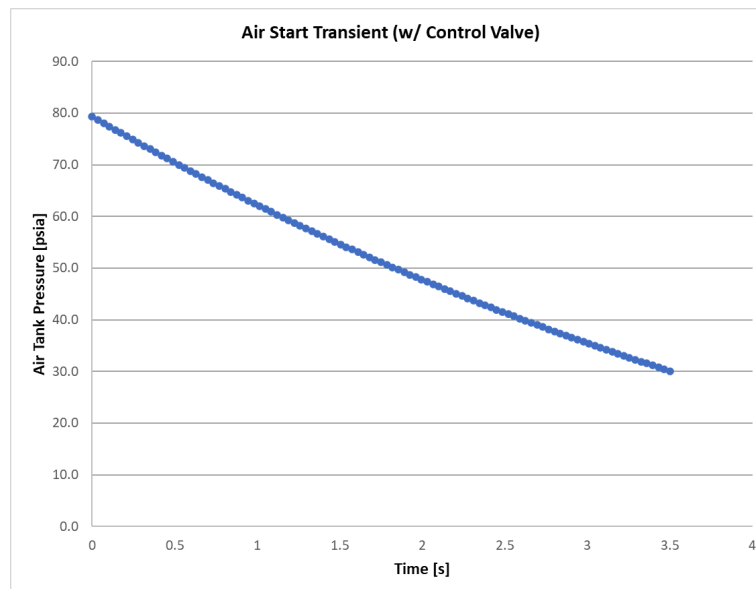


**Figure 36.** Air start transient analysis with a control valve

Figure 36 shows that, with a control valve, the compressed air system could run for 3.5 seconds instead of 0.5 seconds.

The control valve was then selected through an analysis of valve  $C_v$  values. Kimray was chosen as the brand of valve since they provided detailed information on flow values and an equation that could be used to verify the flow of every valve in stock.

$$C_v = \frac{41666Q\sqrt{GT}}{834C_f P_1 (y - 0.148y^3)} \quad y = \frac{1.63}{C_f} \sqrt{\frac{\Delta P}{P_1}} \leq 1.50$$

**Figure 37.** Equations used to calculate the  $C_v$  values of the control valve<sup>7</sup>

Using the equations in Figure 37, the  $C_v$  values could be calculated at every time step in the transient flow analysis. This allowed for the selection of a control valve that fell within the range of the calculated values, which were minimum 2.3 and maximum 5.4.

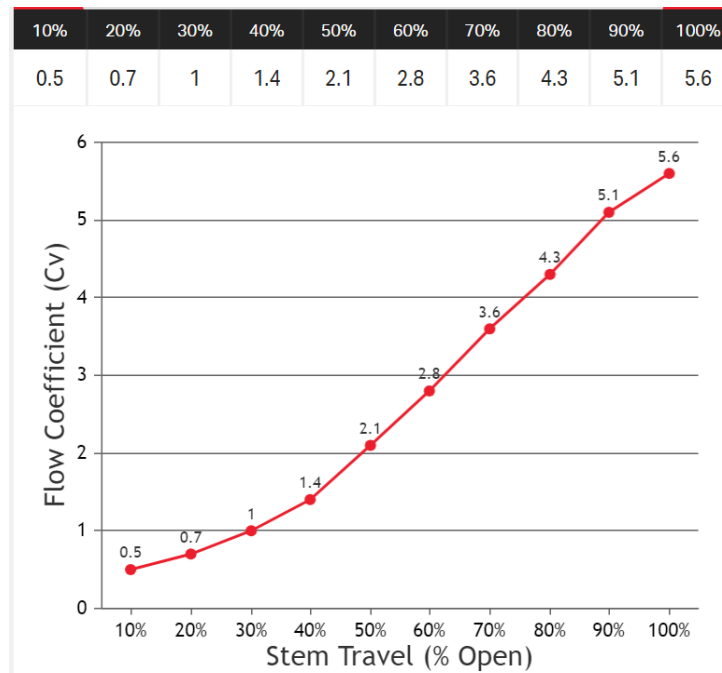


**Figure 38.** Kimray MXC valve flow coefficients at % Open<sup>8</sup>

Using these values, the Kimray MXC control valve was selected, as shown in Figure 38. A control algorithm could be used to open the valve based on the transient analysis.

<sup>7</sup> “Gas Sizing | Kimray,” *kimray.com*. [https://kimray.com/sizing-calculator/gas-sizing?\\_gl=1](https://kimray.com/sizing-calculator/gas-sizing?_gl=1) (accessed Apr. 28, 2024).

<sup>8</sup> “MXC | Kimray,” *kimray.com*. <https://kimray.com/product/mxc> (accessed Apr. 28, 2024).

### 4.11 Fuel Flow Sizing

The propane system selection began with a simple analysis of the required mass flow rate of the system and the expected length of the lab exercise. Assuming the lab exercise would be no longer than 2.5 continuous hours, the fuel flow rate of  $0.007 \frac{\text{lbm}}{\text{s}}$  was used to determine that 63 pounds of propane were needed to run the system for that amount of time. Figure 39 shows the propane conditions and flow rate.

Fuel Flow =	0.007	lbm/s
Ambient Temp =	520	R
Tank Pressure (sat. conditions) =	107.7	psia
Vapor Density =	1	lb/ft <sup>3</sup>
Volume Flow =	0.007	ft <sup>3</sup> /s
Lab length =	2.5	hr
	9000	s
Propane needed =	63	lbm
Volume Flow =	11.9	lpm
	83.5	slpm

**Figure 39.** Fuel flow parameters and calculations

Two 30-pound propane tanks were selected to provide the correct amount of fuel and meet the size constraints of the cart design. In order to ensure constant fuel flow, an automatic propane regulator was selected that would switch from one tank to the other when the first lost pressure. A valve to control the flow of propane was selected based on the desired constant flow rate (83.5 slpm). For the precise control required with the fuel flow, a needle valve (with a max flow rate of 240 slpm) was used. As described in *Section 4.8.2*, the opening of this valve would be controlled by a LabVIEW program that references the combustor exhaust temperature.

## 5 Feasibility Analysis

### 5.1 Combustion Chamber Compressor Flow Analysis (no combustion)

The primary goal of computing a flow simulation is to visually determine the streamflow characteristics from the compressor and its interaction inside the combustion chamber. The initial condition for the compressor inlet flow was determined by the compressor map of the turbocharger. When the turbocharger is running at  $\sim 70,000$  RPM, the compressor map from Figure 9 shows an airflow rate of  $\sim 0.264$  kg/s. For the fuel injector, only the trajectory of the propane fuel was observed with an estimated mass flow rate of 0.05kg/s through a hole 10mm in diameter. The simulation was done using SolidWork's Flow Simulation and was divided into two results: the flow characteristics inside the flame tube and the flow characteristics outside the

flame tube. The fifth revision of the combustion chamber and flame tube design was used for this demonstration (shown below).

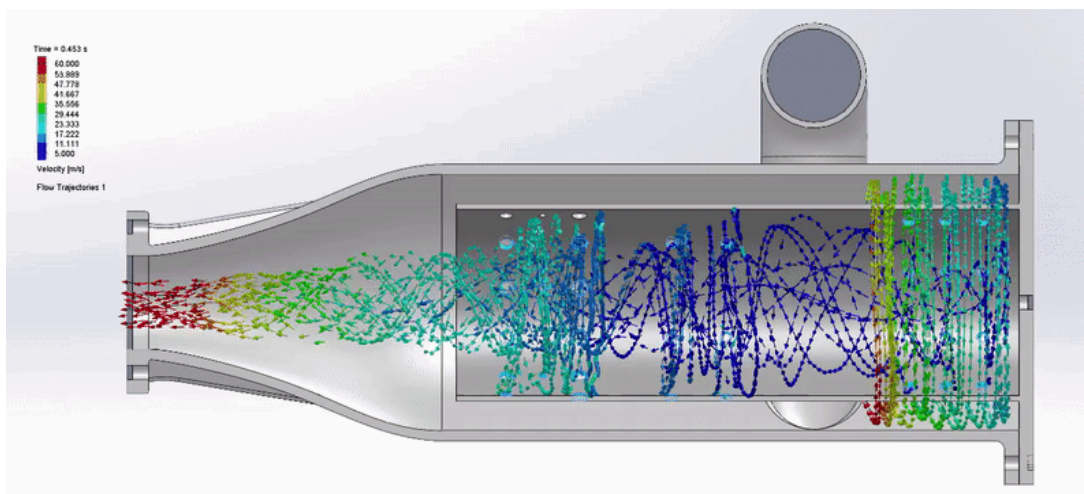


**Figure 40.** Inner flame tube streamflow simulation results (gradient shows velocity)

Starting around the primary zone, high velocity flow from the compressor can be seen circulation outside the flame tube. Contrastingly, inside the flame tube, low velocity flow from the fuel injector can be seen circulating. This demonstrates a clear separation between the high velocity and low velocity air stream which should improve flame preservation.

Around the secondary and tertiary zones, higher velocity streams from the compressor can be seen entering the flame tube to help control incomplete combustion and temperatures. Note however, that the granularity of the mesh generated of the CAD model was not detailed enough to demonstrate micromixing about each hole in the flame tube.

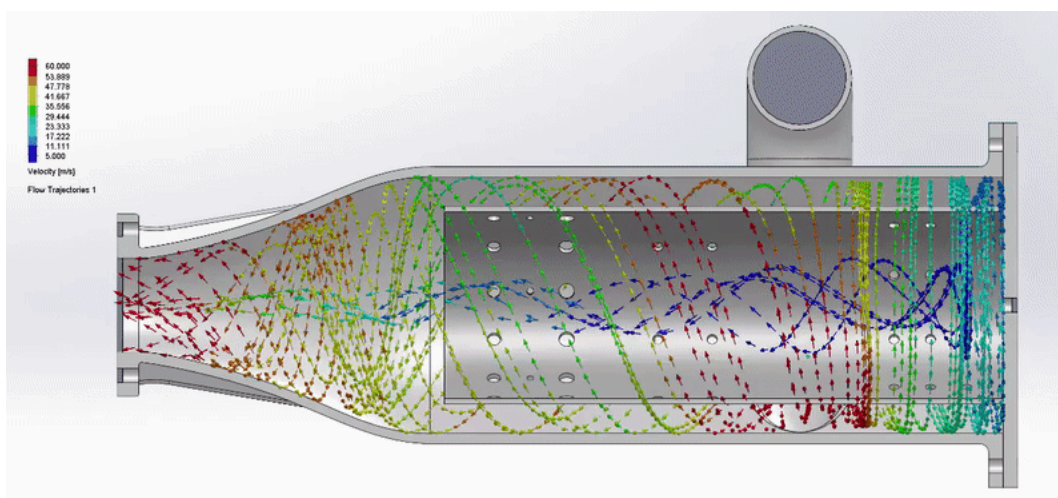


**Figure 41.** Outer flame tube streamflow simulation results (gradient shows velocity)

As intentionally designed, the inlet into the combustion chamber from the turbocharger compressor was off centered to encourage the circulation around the flame tube rather than the airflow splitting then conflicting if centered along the symmetrical axis. As seen in the figure above, the airflow is circulating only in a clockwise direction as it flows around the flame tube. As a result, there are very few areas of loss where a flowstream is colliding with another or small pockets of unwanted circulation.

## 5.2 Revised Combustion Chamber Compressor Flow Analysis (no combustion)

Under similar conditions to the previous combustion chamber a greater focus was emphasized in extracting detail from the CFD model. Specifically, the air flow pressure distribution around the inner flame tube as well as the micro-mixing in the primary zone was the key focus. To achieve this, a higher mesh density was needed which contributed to a greater simulation run time.

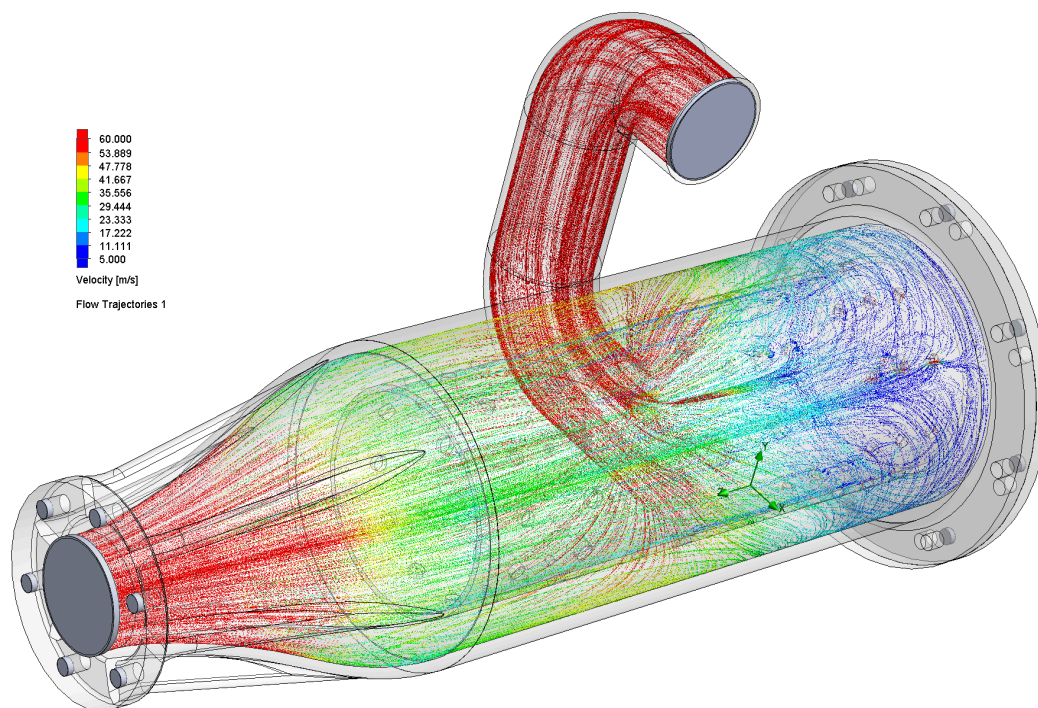


**Figure 42.** SolidWorks CFD velocity air flow distribution around flame tube design 5 (velocity range: 5–60 m/s)

From the simulation results seen in the above figure, greater detail over the volume of the combustion chamber was achieved over the previous simulation iterations. As seen, the rear portion of the chamber experienced lower velocities (~5–17 m/s seen in blue). This was achieved by moving the inlet forward to be placed ahead of the primary zone of the flame tube. While this makes for energetic losses around the rear of the chamber which disturbs the continuous air flow

further down the combustor, the lower velocities will help prevent the blowout of the flame inside.

The advantage of a finer mesh to allow for more detail in the analysis is shown when examining the air flow streams along the primary zone into the flame tube. As seen in the figure below, high velocity air (seen in red) enters through the small perforations in the primary zone which is then expanded into the lower pressure region which reduces its velocity (transition into blue). Surrounding the holes shows spirals of air streams which represent the air circulations as described in *Section 2.5*.

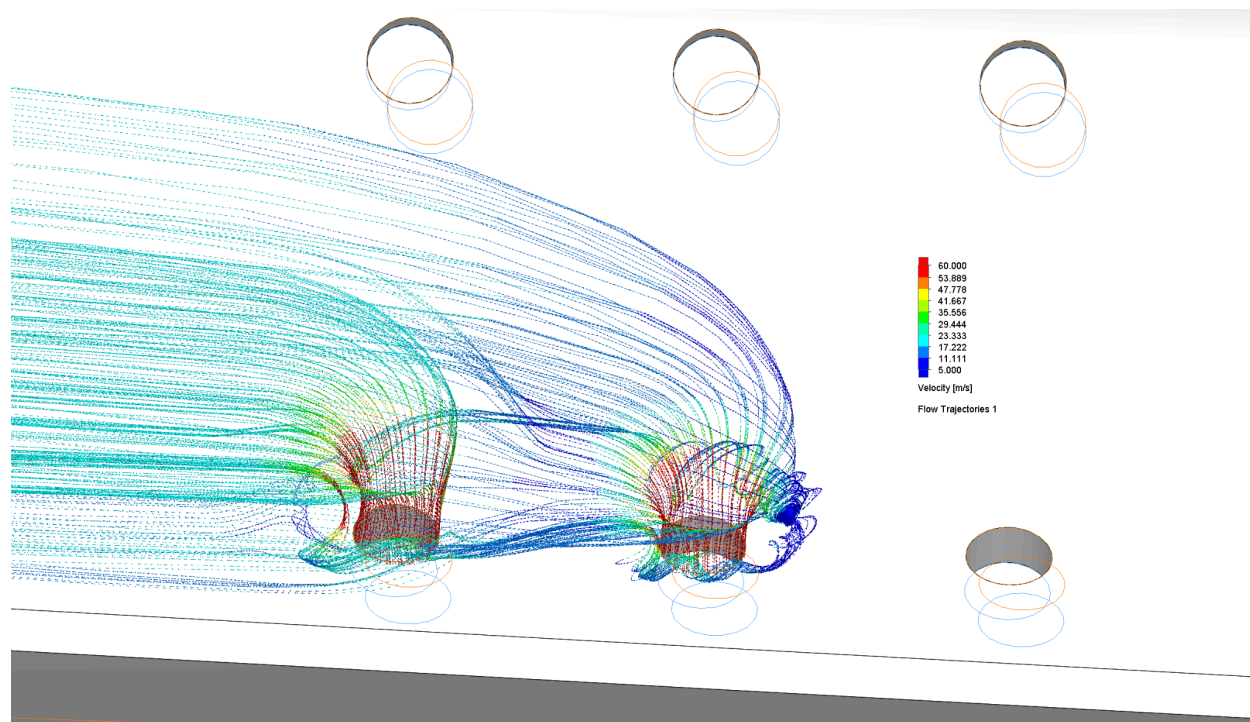


**Figure 43.** SolidWorks CFD flow stream analysis of the micro-mixing circulation around the primary zone holes inside the flame tube

### 5.3 Combustion Analysis of the Flame Tube Design

Concerning the simulation tools available to represent the combustion of propane, few options were available. The software used for the project was SimFlow CFD which allows for spray combustion of the fuel source. While the software fulfills the purpose of demonstrating and calculating the pressure and temperature gradient of the combustion in accurate time, it cannot simulate the compressor air flow and the free trial of the software only allows a mesh node limit of 200,000. Under these constraints, any conclusions on the thermodynamic characteristics are not to be taken realistically. Nevertheless, a 2-day calculation was conducted for a simulation time of 0.01 seconds.

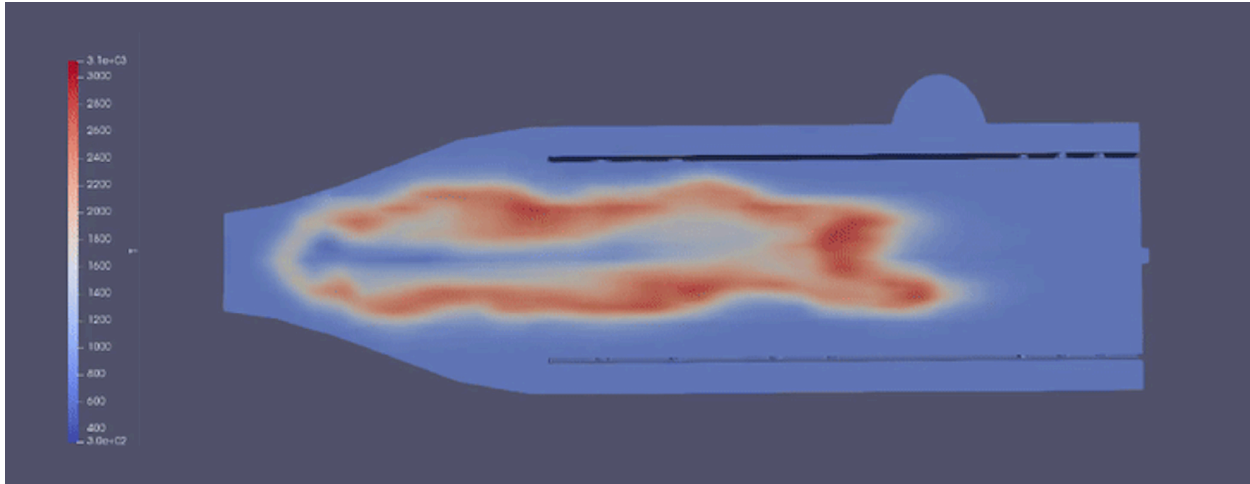


**Figure 44.** SimFlow CFD combustion simulation of propane in the flame tube

The results from the simulation aren't conclusive as the airflow from the compressor supplying the air to the flame tube isn't represented. Thus the interaction and use of the flame tube shows no evidence of influencing the combustion process. To properly evaluate the performance of the flame tube and the combustion chamber, a prototype model will need to be constructed and tested.

## 6 Conclusion

Through the process, the team learned a lot about how to manage the work for a complex system. Going into the project, none of the members were very familiar with the subsystems they were tasked with designing, which forced each member of the team to spend a considerable amount of time on research. On top of that, each of the subsystems were very different, so a large part of the work was figuring out how to integrate everything efficiently. When one person's design or the operating conditions changed, the design of other subsystems needed slight alterations, which required good communication among team members. The team learned a lot about how to keep everyone on track so the overall design of the system could progress.

The project required each team member to carry out numerical analyses and then design or source components based on the results. This process gave the team experience in using knowledge from basic engineering courses (pulley dynamics, heat transfer, thermodynamics, structural analysis, flow simulation, etc.) in a more practical way. The team needed to learn how to combine all of these analyses into one cohesive, functioning system.

While the entire system was not tested to check its feasibility, the team was able to source the most important parts for every subsystem based on results from spreadsheet calculations and flow simulations. The team delivered a full CAD model of the system for assembly purposes, line diagrams for the electrical and cooling systems, and a BOM that details the components for each subsystem and where to source them or how to manufacture them. The

main parts of the system that did not receive a full analysis were the circuitry and the coding aspects. Future teams should focus on creating circuit diagrams to ensure safe power transfer to all components, on creating the control interface in LabVIEW to draft system start-up and shut-down sequences, and on creating a detailed fuel injection and ignition sequence.

## 7 Further Works

### 7.1.1 Hybrid Turbochargers (MGU-H)

A different approach to the pulley system for generating power is to attach a generator/motor that runs in series one-to-one with the turbocharger shaft. This design is advantageous because the turboshaft isn't exposed (for safety), the area of the inducer into the compressor is not restricted, the setup for the bearing system is simplified, and the turboshaft isn't elongated to the same degree. A system such as this does pose complications in its design in that the generator/motor must run at the same RPM as the turbocharger (70,000+ RPM). Currently on the market, no such product exists at the consumer level. This technology predominantly exists in the competitive automotive racing industry, most known in Formula 1.

Formula 1 has pioneered the design of the “hybrid” turbocharger with the 2014 technical regulations. It was under the Mercedes F1 team that first introduced the “split” turbocharger design into the sport where the motor-generator unit (MGU-H) (H for “heat”) sits between the compressor and the turbine of the turbocharger.<sup>9</sup>

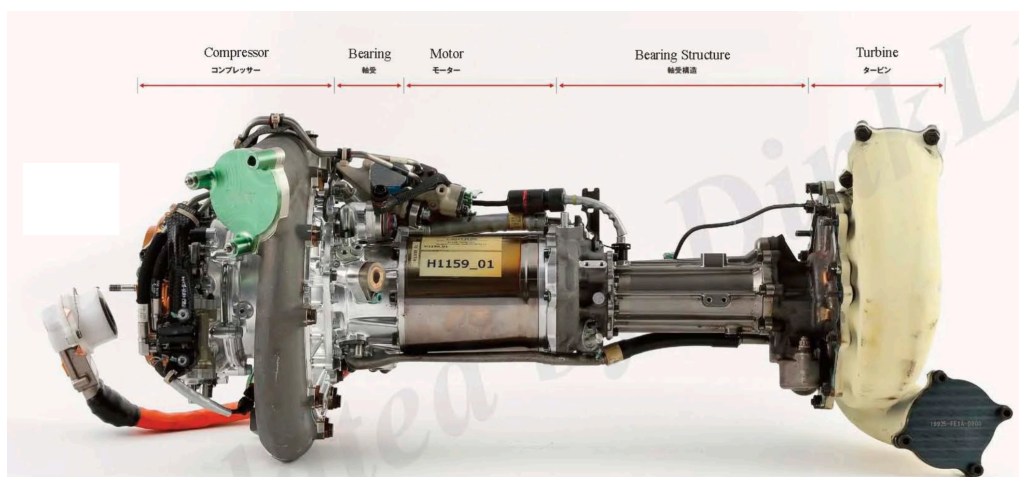


**Figure 45.** Honda Formula 1 Split Hybrid Turbocharger

Splitting the turbine from the compressor decreases the amount of heat-soak into the compressor allowing the air flowing into the combustor to be more dense as it is cooler. It also doesn't restrict the compressor inducer compared to the pulley design previously mentioned

<sup>9</sup> MotorFan, “MGU-H Assy: A Longer Axis for a Longer Turbocharger”, *Honda Power Unit Development*, 2021.

which would improve the efficiency and reduce thermal stress on the system. This design was the inspiration for this project's design.

### 7.1.2 Electric Generator Concept in Series (MGU-H)

As previously stated, the design philosophy for the electric motor/generator unit was inspired by the hybrid turbochargers from Formula 1. While this approach is far simpler than the pulley design previously mentioned, it requires more precise and more advanced manufacturing and simulation to achieve the goal of power generation. However, in the confines of the project's resources and time constraint, our goal is not to manufacture the integrated MGU-H by the end of the project. Instead, our goal is to only design and simulate a working system.

Based on the designs of hybrid turbochargers from Formula 1, this integrated MGU-H is intended to sit between the compressor and turbine side with the motor directly driving and generating power in series with the turboshaft (seen in the Figure below). This design tightly packs the power generator with the whole system and is far simpler than a belt and pulley RPM reduction system as well as being safer. Since the 70,000 RPM turboshaft isn't exposed out of the compressor side, the shaft doesn't interfere with the indicer area of the compressor, meaning it won't affect the efficiency of compression.

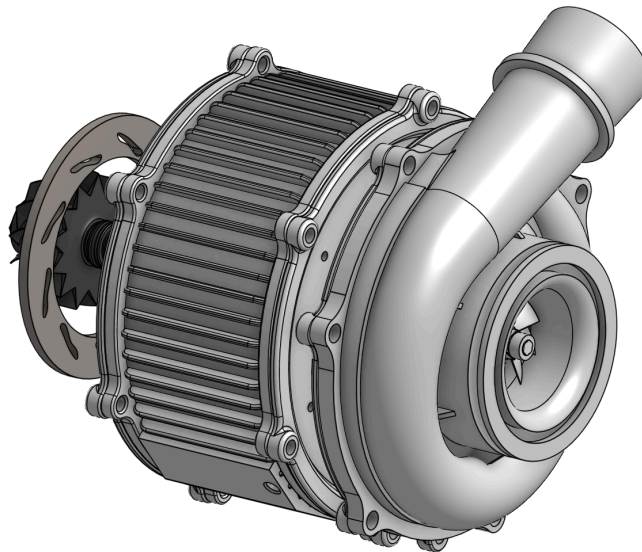


**Figure 46.** Modeled Design of Integrated MGU-H with Compressor

Most designs of high RPM motor generators take advantage of an induction motor rather than a synchronous motor. At speeds above 6500+ RPM, the rotor core of a synchronous motor which includes the induction coils, cannot withstand the centrifugal forces under sustained loads. Thus, a more simplified induction motor with the permanent magnets (PMs) as the rotor core is

more suited for sustained high RPM running.<sup>10</sup> If the number of poles were to double, the maximum RPM of the motor would be halved. Thus reducing the number of rotor poles allows for higher RPM under the assumption that the desired switching frequency of ~1.2kHz can be achieved without incurring losses due to heat.

To help solve this problem, the outer casing was designed with a fin array to dissipate heat as well as two port holes for water cooling. Slots running about the circumference of the stator core allows for a greater surface area for the water to cool the core (see the Figure below). This is an important aspect of the design as overheating a motor causes an increase in resistance in the stator coils which affects the flux density, wear the mechanical bearings, and can alter the PM field strength.

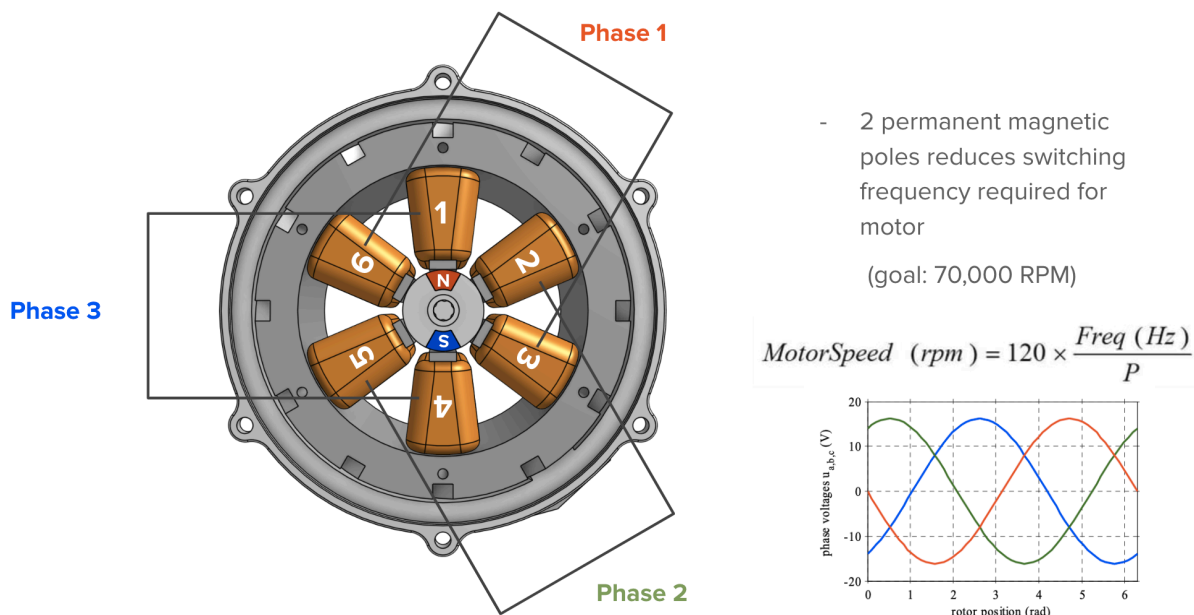


**Figure 47.** MGU-H Internal Design Setup (2 pole, 3-phase induction)

The figure above shows an untested design of a motor/generator unit containing a 2-pole PM rotor core encased in a sleeve and a 3 phase slotted stator core. At either end are spindle roller bearings that would be designed to run past the rated RPM of the turbocharger (70,000+ RPM). While solutions such as magnetic or journal bearings pose greater efficiencies, since the mechanism is likely to run a few times per year for a few hours, mechanical bearings are the cheaper solution that still suits the needs of the project.

## 7.2 Scale Prototype Combustion Chamber Model

As simulation tools are not available to accurately analyze the performance of the flame

<sup>10</sup> C. Zwyssig, J. W. Kolar, W. Thaler and M. Vohrer, "Design of a 100 W, 500000 rpm permanent-magnet generator for mesoscale gas turbines," Fourtieth IAS Annual Meeting. Conference Record of the 2005 Industry Applications Conference, 2005., Hong Kong, China, 2005, pp. 253-260 Vol. 1, doi: 10.1109/IAS.2005.1518318.

tube design on metrics of efficiency or energy output, constructing at least a scaled model will help to give a better understanding of the combustion process. Thus, with a budget of ~\$300, a clear combustion chamber with a quartz glass flame tube was modeled off of the specialized flame tube design seen in previous sections (shown below).

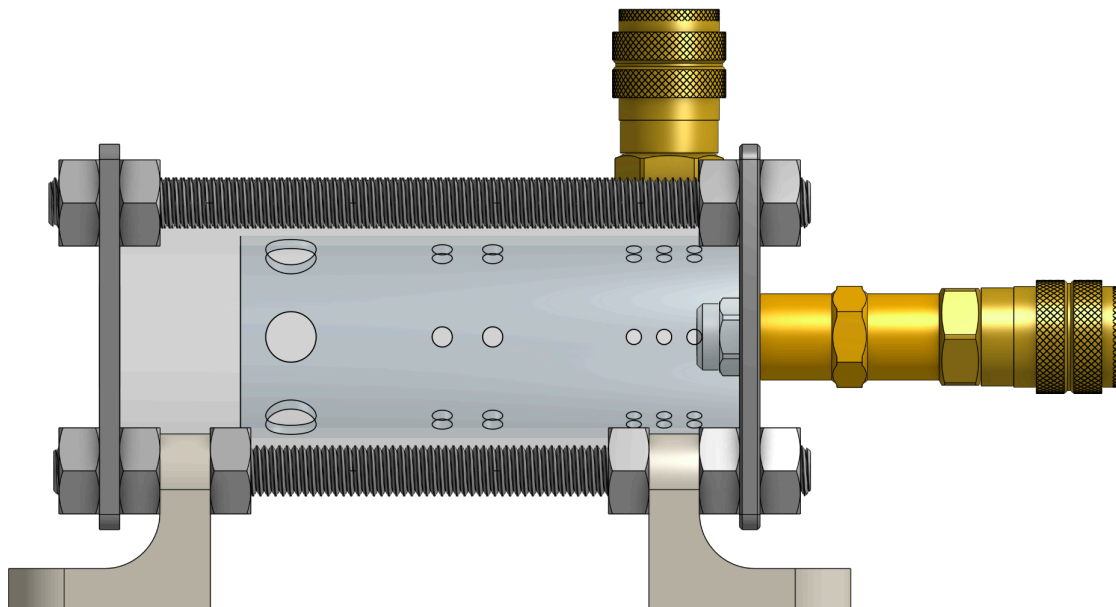


**Figure 48.** Scaled prototype combustion chamber with quartz glass flame tube and carbon steel retaining plates with quick disconnect fittings for compressed air and propane lines

The transparent nature of the prototype was designed to be analyzed under the view of a camera to better understand the interaction of the high velocity air flow and the inner flame tube. The nozzle type is a wide 20° spray injection linked to a quick disconnect fitting for the propane source (the same intended for the full scale build). The upper fitting is meant for a compressed air source of at least 100 PSI to supplement for the compressor of the turbocharger. The threaded rods link the two carbon steel plates meant to be removable in the event of testing multiple quartz glass flame tube designs. Unfortunately, due to the brittleness of quartz glass as well as the scale (1:3) compared to the full scale model, the holes are not to scale but are represented in their localized dimension and location. Currently, a scale model has been made and a test operation is underway to visually represent the capabilities of this design of a combustion chamber. For a performance metric to compare various designs, a mock instrumentation system with pitot tubes and air flow meters are needed to find the optimal flame tube design.

## References

- Al Ameen Hassana, Bavanitha Sivasubramaniamb, Daphne Miriam, Hephzin K Varghese, G. Dinesh Kumar , V. Paulson, “Modeling and Simulation of Combustion Chamber for a Turbocharger Jet Engine”, AIP Publishing, 2022.
- “Aeolus: Combustion Chambers.” *JetX Engineering*, [www.jet-x.org/a4.html](http://www.jet-x.org/a4.html). Accessed 12 Oct. 2023.
- Arnedo, Manuel Soler. “6.2.4: Combustion Chamber.” *Engineering LibreTexts*, Libretexts, 21 Jan. 2022, [eng.libretexts.org/Bookshelves/Aerospace\\_Engineering/Fundamentals\\_of\\_Aerospace\\_Engineering\\_\(Arnedo\)/06%3A\\_Aircraft\\_propulsion/6.02%3A\\_The\\_jet\\_engine/6.2.04%3A\\_Combustion\\_chamber](https://eng.libretexts.org/Bookshelves/Aerospace_Engineering/Fundamentals_of_Aerospace_Engineering_(Arnedo)/06%3A_Aircraft_propulsion/6.02%3A_The_jet_engine/6.2.04%3A_Combustion_chamber).
- C. Zwysig, J. W. Kolar, W. Thaler and M. Vohrer, "Design of a 100 W, 500000 rpm permanent-magnet generator for mesoscale gas turbines," Fourtieth IAS Annual Meeting. Conference Record of the 2005 Industry Applications Conference, 2005., Hong Kong, China, 2005, pp. 253-260 Vol. 1, doi: 10.1109/IAS.2005.1518318.
- H. Arimizu, M. Ebisu, K. Osako, N. Hayashi, T. Himeno, “Development of Variable Geometry Turbocharger for Gasoline Engine.” Mitsubishi Heavy Industries, 2012.
- John Kyle Thoma, Daniel Shehan, Benjamin Naravage, Jacob Melvin, “Design, Fabrication, and Testing of an Automotive Turbocharger-Based Gas Turbine Engine”, *California Polytechnic State University, San Luis Obispo, June 2010*.
- Lefebvre, Arthur H., and Dilip R. Ballal. “Basic Considerations.” *Gas Turbine Combustion Alternative Fuels and Emissions*, Taylor & Francis, Boca Raton u.a., FL, 2010, pp. 15–17.
- MotorFan, “MGU-H Assy: A Longer Axis for a Longer Turbocharger”, Honda Power Unit Development, 2021.

Moran, Michael J., Howard N. Shapiro, Daisie D. Boettner, and Margaret B. Bailey.

*Fundamentals of Engineering Thermodynamics*. 8th ed. Wiley, 2014.

“U.S. Energy Information Administration - EIA - independent statistics and analysis,” How electricity is generated - U.S. Energy Information Administration (EIA), <https://www.eia.gov/energyexplained/electricity/how-electricity-is-generated.php> (accessed Apr. 28, 2024).

## Appendices

### Bill of Materials (BOM)

#### Combustion Chamber and Motor-Pulley

Part No.	Product No.	Product Description	QTY	Price Per	Total Price	Notes
CC001	26666	Combustion Chamber (main body)	1	\$794.93	\$794.93	
CC001	mp-00000225	Combustion Chamber (base plate)	2	\$283.71	\$567.42	
CC001	mp-00000225	Combustion Chamber (nozzle mount)	1	\$131.11	\$131.11	
CC002	STW-5SS-2	Flame Tube	1	\$92.15	\$92.15	
CC003	3009	Gasket Seal	1	\$11.79	\$11.79	
CC005	BPR4ES	Copper Spark Plugs	1	\$7.79	\$7.79	
CC006	90447A270	M10 Hex Bolts	1	\$7.95	\$7.95	
CC007	90593A008	M10 Hex Nuts	1	\$8.28	\$8.28	
CC008	10408	Combustion Chamber Holder	1	\$138.93	\$138.93	Made from 24"x48"( $\frac{1}{4}$ " ) A36 Steel Plate
MPA001	U10P1D	Motor Generator (10Hp)	1	\$1,475.00	\$1,475.00	
MPA002	91177A220	Steel Threaded Rods and Hex Nuts	4	\$9.71	\$38.84	Includes Hex Nuts
MPA003	6204K561	Heavy Duty V-Belt Pulley (11.75 in)	1	\$99.46	\$99.46	
MPA004	6204K551	Heavy Duty V-Belt Pulley (10.75 in)	1	\$95.85	\$95.85	
MPA005	6204K141	Heavy Duty V-Belt Pulleys (2.55 in)	1	\$19.28	\$19.28	
MPA006	6204K135	Heavy Duty V-Belt	1	\$16.16	\$16.16	

		Pulleys (2.5 in)				
MPA007	5909K33	Needle-Roller Thrust Bearing for 3/4" Shaft	3	\$3.92	\$11.76	
MPA007	5909K46	Needle-Roller Thrust Bearing for 3/4" Shaft (washer)	6	\$1.35	\$8.10	
MPA009	6675K16	High-Speed Flange-Mounted Linear Sleeve Bearing (1 ¼" shaft)	1	\$151.75	\$151.75	Ceramic bearings
MPA010	6675K12	High-Speed Flange-Mounted Linear Sleeve Bearing (¾" shaft)	2	\$72.76	\$145.52	Ceramic bearings
MPA011	19924	Carbon Steel Round Spacer (mid shaft)	1	\$12.41	\$12.41	
MPA012	10057	Carbon Steel Round Spacer (turbo shaft)	1	\$6.04	\$6.04	
MPA013	mp-00000337	Aluminum 6061-T651 Front Plate	1	\$122.34	\$122.34	
MPA014	mp-00000337	Aluminum 6061-T651 Rear Plate	1	\$122.34	\$122.34	
MPA015	1098	Aluminum 6061 Round Bar (motor shaft)	1	\$76.25	\$76.25	
MPA016	4796	Carbon Steel Round Bar 1018 (turbo shaft)	1	\$20.83	\$20.83	
MPA017	4796	Carbon Steel Round Bar 1018 (mid shaft)	1	\$20.83	\$20.83	
MPA018	92314A296	18-8 Stainless Steel Hex Head Screws	1	\$10.16	\$10.16	Bearing Screws
MPA019	92240A108	18-8 Stainless Steel Hex Head Screws	1	\$8.68	\$8.68	Bearing Screws

**Oil Loop**

Part No.	Product No.	Product Description	QTY	Price Per	Total Price	Notes
OC-0001	TS-0801-100 2	Oil Pressure Regulator (40psi)	1	\$136.00	\$136.00	regulates oil pressure to 40psi
OC-0002	B08T696D45	Oil Impeller Pump (12V)	1	\$70.00	\$70.00	
OC-0003	B3-23A	Oil-Water Heat Exchanger	1	\$171.23	\$171.23	1/2" MNPT
OC-0004	HM1248	Oil Reservoir	1	\$31.59	\$31.59	2.5L
OC-0005	B0BFD6RK6 G	3/8" ID Hose	1	\$13.59	\$13.59	10ft
OC-0006	B0BZHXS6Y 9	1/2" Hose	2	\$13.99	\$27.98	10ft
OC-0007	5346K56	1/2" FNPT to 3/8" Barb	1	\$22.25	\$22.25	HX to 3/8" hose, pack of 5 only
OC-0008	KB-6.6lTOD-B A	Oil Drain Adaptor	1	\$30.95	\$30.95	-10 AN, attaches to oil drain
OC-0009	SUM-220768B	-10AN to 1/2" Barb Adaptor	1	\$5.09	\$5.09	Connect to oil drain adaptor
OC-0010	5346K57	1/2" FNPT to 1/2" Barb	1	\$4.22	\$4.22	Attach to HX oil inlet
OC-0011	E.I. BARB 302	1/8" MNPT to 1/2" Barb	1	\$8.45	\$8.45	Oil feed is 1/8" NPT

**Coolant Loop**

Part No.	Product No.	Product Description	QTY	Price Per	Total Price	Notes
CO-0001	ALLOYWOR KS-1074	Radiator-Fan	1	\$229.00	\$229.00	
CO-0002	SFDP1-030-0 45-33	DC Water Pump (12V)	1	\$49.99	\$49.99	3.0gpm

CO-0003	12346290	General Motors ACDelco DEX-Cool Coolant Antifreeze	1	\$33.40	\$33.40	
CO-0004	B0BZHXS6Y 9	1/2" ID Hose (10ft)	2	\$13.99	\$27.98	
CO-0005	5346K57	1/2" FNPT to 1/2" Barb	2	\$4.22	\$8.44	To attach to HX inlet
CO-0006	5350K79	1/4" MNPT to 1/2" Barb	2	\$1.39	\$2.78	Attach to turbo inlet
CO-0007	5350K82	1/2" Barb to 1/2" MNPT	2	\$2.78	\$5.56	
CO-0008	SS0190000	1-1/4" FNPT to 1/2" FNPT Reducer	1	\$9.99	\$9.99	Attach 1/2" barb and 1-1/4" barb
CO-0009	B09N9BZW QN	1-1/4" MNPT to 1-1/4" Barb	1	\$16.99	\$16.99	
CO-0010	B095H7X2Q 7	1-1/4" ID Hose (3.3ft)	1	\$14.99	\$14.99	
CO-0011	B09N998P5N	1-1/2" MNPT to 1-1/2" Barb	1	\$18.99	\$18.99	
CO-0012	B01MFC327 H	1-1/2" FNPT to 1/2" FNPT Reducer	1	\$9.99	\$9.99	Attach 1-1/2" barb and 1/2" barb
CO-0013	B095HCXC W5	1-1/2" ID Hose (3.3ft)	1	\$17.99	\$17.99	

### Cart Extrusions

Part No.	Product No.	Product Description	QTY	Price Per	Total Price	Notes
CA-038	47065T426	T Slot 38 Inch 6105 Aluminum	8	\$56.04	\$448.32	Original Length Actually 48 Inch
CA-029	47065T629	T Slot 29 Inch 6105 Aluminum	17	\$42.94	\$729.98	Original Length

						Actually 36 Inch
CA-060	47065T857	T Slot 60 Inch 6105 Aluminum	4	\$69.13	\$276.52	n/a
CA-010	47065T856	T Slot 10 Inch 6105 Aluminum	2	\$16.75	\$33.50	Original Length Actually 12 Inch
CA-015	47065T627	T Slot 15 Inch 6105 Aluminum	8	\$29.84	\$238.72	Original Length Actually 24 Inch
CA-007	47065T101	T Slot 7 Inch 6105 Aluminum	2	\$8.67	\$17.34	Original Length Actually 12 Inch (Single Rail, 1 Inch Thick)

### Cart Fasteners

Part No.	Product No.	Product Description	QTY	Price Per	Total Price	Notes
CF-001	47065T893	Larger Gusset Fastener Anodized 6105 Aluminum	78	\$25.63	\$1,999.14	Comes in single piece
CF-003	47065T253	T Slot Framing Corner Bracket Anodized 6105 Aluminum	55	\$12.03	\$661.65	Comes in single piece
CF-004	47065T147	T Slot Framing Fastener End Feed With 2 Holes Zinc Plated Steel	34	\$6.12	\$208.08	Fastener Installation Type: End Feed Fastener Thread Size: 1/4"-20

						Fastener Thread Length: 1/2" Fastener Drive Style: Hex; Comes in pack of 4
CF-005	3136N122	Mesh Fasteners Anodized Aluminum	4	\$19.15	\$76.60	For use with mesh needs extra 1/4 screws
CF-006	47065T255	1 Inch Fastener 6105 Aluminum	4	\$9.23	\$36.92	Comes with two screws, 1/4 inch screws
CF-007	90128A619	3/8 - 16 Screws Zinc Plated Steel	1	\$7.90	\$7.90	Comes in pack of 25
CF-008	90128A245	1/4-20 (3/4" Length) Screws Zinc Plated Steel	1	\$12.32	\$12.32	Comes in pack of 50
CF-009	95462A029	Nuts for Pipe Mounting Zinc Plated Steel	1	\$8.95	\$8.95	Comes in pack of 100

### Pipe and Tubes

Part No.	Product No.	Product Description	QTY	Price Per	Total Price	Notes
PT-001	487	Pipe Tubing A513 - Type 5	1	\$200.28	\$200.28	72 Inch Steel Tube. Cut to size as needed for the entire pipe assembly. OD = 2.5" and ID = 2.37"

PT-002	SKU 21018-D	Elbow Tube 304 Stainless	5	\$22.50	\$112.50	Tight Radius 90 Degrees. Need for each corner bend.
--------	-------------	-----------------------------	---	---------	----------	---

### Misc Cart Parts

Part No.	Product No.	Product Description	QTY	Price Per	Total Price	Notes
CP-001	1248	Aluminum Plate for Motor Mount 6061 T651	1	\$92.67	\$92.67	Originally 12" x 24". Cut to size based on need.
CP-002	n/a	Bottom Panel of Cart A36 Carbon Steel	1	\$101.02	\$101.02	n/a
CP-003	9993	Riser Plates A36 Carbon Steel	1	79.53	79.53	Originally 24" x 24". Cut to size based on need
CP-004	SKU 1232	Control Box PVC	1	\$124.29	\$124.29	Slightly smaller than CAD model version. Also differs from the actual design and likely will need custom mount that hasn't been designed.
CP-005	9610	Plate For Propane Tanks A36 Carbon Steel	1	\$106.75	\$106.75	CAD model is not representativ e for final

						use. Simplest support recommended is to use the plate of the following dimension (30"x14") or situate in a way that the propane tank can sit on the extrusion itself.
CP-006	n/a	Aluminum Block for Turbo Mount 6061	1	\$229.75	\$229.75	This block will have to be machined into the right shape.
CP-007	47065T901	Mesh Panel Anodized Aluminum	1	\$66.48	\$66.48	Originally 2' x 2'. Cut to size for two mesh panels
CP-008	47065T591	Cart Handle Aluminum	2	\$46.02	\$92.04	The CAD version is more of a visual representation
CP-009	9949T99	Cart Casters Zinc Plated Steel and Rubber	4	\$89.45	\$357.80	n/a

### Air Start System

Part No.	Product No.	Product Description	QTY	Price Per	Total Price	Notes
----------	-------------	---------------------	-----	-----------	-------------	-------

AS-0001	H-3862	Air Tank Compressor	1	\$1,020.00	\$1,020.00	30 gallon, 135 psi max, 1/4" NPT outlet
AS-0002	MXC	Electronic Control Valve	1	Quote Needed		
AS-0003	KA7506	Analog MXC Module	1	Quote Needed		4-20mA controlled, order this as an option with the above
AS-0004	B07VTRVD7 5	0-5V to 4-20mA	1	\$9.99	\$9.99	Convert 0-5V into 4-20mA for valve
AS-0005	46511	1/4" NPT Hose	1	\$14.79	\$14.79	Connect to control valve through bushing
AS-0006	K414-1604	1/4" NPT to 1" NPT Bushing	1	\$4.53	\$4.53	So much pressure loss...
AS-0007	FA-UFW16- NPT-12	1" MNPT Hose	1	\$28.02	\$28.02	Both connections MNPT, 12" long
AS-0008	WB-N16-SS3 04	1" FNPT Weld-on Bung	1	\$12.99	\$12.99	

### Fuel

Part No.	Product No.	Product Description	QTY	Price Per	Total Price	Notes
F-0001	YSN301	30lb Propane Tank	2	\$72.99	\$145.98	
F-0002	KT12ACR6	Propane Changeover	1	\$37.18	\$37.18	Automatic changeover, Inlets are

						1/4" SAE inverted flare and outlet is 3/8" NPT female pipe thread
F-0003	LX-1208	1/8" MNPT Hose	2	\$15.29	\$30.58	1) Regulator outlet to control valve inlet 2) Control valve outlet to nozzle
F-0004	9035S-02-02	1/8" FNPT to 1/8" Male BSPP	2	\$3.26	\$6.52	Connects to control valve inlet
F-0005	4464K262	3/8" MNPT to 1/8" FNPT	1	\$3.75	\$3.75	Connects to regulator outlet and 1/8" hose
F-0006	9151K61	1/8" FNPT to FNPT Connector	1	\$2.03	\$2.03	
F-0007	B07FZSHT9 N	1/8" NPT Male to M8 M8X1 M8X1.0 Female	1	\$10.98	\$10.98	90 deg bend
F-0008	B08111XPB7	Propane Spray Nozzle	1	\$9.98	\$9.98	Comes with 4

### Instrumentation and Data

Part No.	Product No.	Product Description	QTY	Price Per	Total Price	Notes
I-0001	PX309-200G 5V	P1, P2, P3, P4, Px Transducer	5	\$368.43	\$1,842.15	1/4" NPT, Px is the transducer downstream of the orifice plate

I-0002	5TC-GG-K-2 4-36-ROHS	T1, T4 Thermocouple	1	\$65.45	\$65.45	Pack of 5, 36"
I-0003	M12KIN-1/8- U-2-B	T2, T3 Thermocouple	2	\$63.91	\$127.82	1/2" NPT
I-0004	M12CM-EXT T-K-SF-3	M12 Connector	2	\$75.52	\$151.04	
I-0005	PG-CTN2-G0 3	P3 Thermal Isolation	1	\$189.89	\$189.89	1/4" NPT
I-0006	SNPT14	P2, P3 Weld-On Bung	2	\$18.70	\$37.40	1/4" NPT
I-0007	LL_1/2NPT_ BUNG	T2, T3 Weld-on Bung	2	\$8.79	\$17.58	1/2" NPT
I-0008	PT6300	P1, P4 Pitot Tube	2	\$42.99	\$85.98	304SS, also measures air speed for mass flow, 15/64" tubing
I-0009	1257559	Clamp Holder	3	\$11.00	\$33.00	Attach to threaded rods
I-0010	1078N138	M6X1 Threaded Rod (150mm)	1	\$6.86	\$6.86	150mm length
I-0011	1078N141	M6X1 Threaded Rod (300mm)	1	\$8.00	\$8.00	300mm length
I-0012	5233K121	6mm ID PVC Tubing (25ft)	1	\$20.75	\$20.75	Attach to pitot tubes and pressure transducers
I-0013	1075T183	6mm Barb to 1/4" FNPT	2	\$12.36	\$24.72	Attach pressure transducer and 6mm ID tubing
I-0014	221030002	Picoturn Controller	1	\$910.00	\$910.00	Output 0.5-4.5V
I-0015	220150012	Picoturn Sensor	1	\$265.00	\$265.00	Connects to controller

I-0016	GM 12643471	Vane Position Sensor	1	\$67.99	\$67.99	Our turbo has one, the wire is just cut before the ECU connection
I-0017	AI-2054	Vane Actuator Cable	1	\$7.29	\$7.29	Should be 12V (maybe 12.6V), need some sort of driver to control variable vanes
C-0001	ENV-0090	Needle Valve, Fuel Flow	1	\$306.00	\$306.00	
C-0002	D5-01-U01	Needle Valve Driver, Fuel Flow	1	\$220.00	\$220.00	24V power, 0-10V signal required
D-0001	NI 782604-01	USB Multifunction DAQ	1	\$331.10	\$331.10	
D-0002	NI 779001-01	Thermocouple DAQ	1	\$770.40	\$770.40	
D-0003	NI 781425-01	USB DAQ Chassis	1	\$561.75	\$561.75	For D-0002

### Electrical

Part No.	Product No.	Product Description	QTY	Price Per	Total Price	Notes
E-0001	AL24V10AT	24V Power Supply (240W)	1	22.99	22.99	
E-0002	LRS-600-12	12V Power Supply (600W)	1	62.99	62.99	
E-0003	D-1410	24V Distribution	1	10.99	10.99	